suppressed the increase of IL-8 and TNFα in THP-1 cells and those of SB203580 and SP600125 had no suppressive effects. These results suggested that an ERK1/2 pathway also plays an important role in the increase of IL-8 and TNFα by butenafine treatment. In contrast, even for the control, the basal IL-8 and TNFα levels in THP-1 cells were suppressed by the pretreatment with U0126 and were increased by the pretreatment with SB203580, suggesting that the basal IL-8 and TNFα levels in THP-1 cells were affected by the MAP kinase inhibitors. In the case of fluconazole, a negative control, the effects of MAP kinase inhibitors on the IL-8 and TNFα levels in THP-1 cells were similar to those of the control (0.1% DMSO). In addition, the levels of ERK1/2 and phospho-ERK1/2 were measured by Western blotting in the presence of polymyxin B to check the potential contamination of LPS. The levels of phospho-ERK1/2 did not change by the addition of polymyxin B (data not shown).

Discussion

THP-1, HL-60, and KG-1 cells are classified as human monocytic cell lines and are useful for studying the differentiation and the activation of immune cells, such as monocytes, macrophages, and immature myelocytes. In the present study, by the treatment with the antifungal drugs terbinafine and butenafine, IL-8 and TNFα release from THP-1 and HL-60 cells was significantly increased compared with the control (Fig. 1A–D). This suggested that terbinafine and butenafine have the ability to stimulate the release of pro-inflammatory cytokines from monocytes, leading to the activation of the inflammatory reaction. In contrast, fluconazole, used as a negative control of terbinafine, had no effects on the cytokine release in THP-1 and HL-60 cells. This result was supported to the previous report that fluconazole had a lower risk of adverse events leading to treatment discontinuation compared with terbinafine (Chang et al. 2007). On the other hand, the cytokine release from KG-1 cells was not increased by the three antifungal drugs (Fig. 1E and F). However, it was reported that even potent inducers, such as LPS, did not increase the cytokine release from KG-1 cells (Teobald et al. 2008).

In our study, at least 25 to 50 μM terbinafine was required to significantly increase IL-8 and TNFα release from THP-1 cells (Fig. 3C and D). It has been reported that the peak plasma concentrations of 3.9 μM appeared at 2 h after a single oral administration of 250 mg terbinafine in humans (Kovarik et al. 1992). Median duration of terbinafine treatment was 12 weeks in 25091 patients of onychomycosis (Hall et al. 1997). Terbinatine was considered a possible or probable cause of 11 (0.04%) serious adverse events. Most likely, the terbinafine-associated hepatic injury in these patients was caused by an idiosyncratic rather than a direct hepatotoxic reaction (van't Wout et al. 1994, Hall et al. 1997). However, immune response-related adverse reactions in human are remained totally unknown. Further study will be necessary to clarify whether oral administration of terbinafine stimulates the release of pro-inflammatory cytokines and chemokines in vivo.

We found that terbinafine stimulates the release of pro-inflammatory cytokines and chemokines from human monocytic cells. The activation of inflammatory responses might be one of the mechanisms underlying the immune-mediated liver injury by terbinafine. On the other hand, the activation of human monocytic cells by other drugs, such as ximelagatran and troglitazone, has been reported recently, although these drugs have been already withdrawn from the market due to idiosyncratic hepatic injury. Ximelagatran increased the release of chemokines from THP-1 cells but the types of released cytokines and the time course of the cytokine release by the drug treatment were different from the case of terbinafine (Edling et al. 2008). In addition, troglitazone increased the mRNA expression levels of pro-inflammatory cytokines and chemokines in THP-1 cells, and some of them were affected by co-culture with human hepatoma Huh-7 cells (Edling et al. 2009). Therefore, measurement of the release of pro-inflammatory cytokines and chemokines from human monocytic cells may be useful to predict adverse reactions to drugs involving immune-mediated hepatic injury.

As reported by Iverson and Uetrecht (2001), the main reactive metabolite of tervinafine is an N-dealkylated product, 7,7-dimethylhept-2-ene-4-ynal (TBF-A). We could not obtain the TBF-A standard chemical in this study. Terbinafine is mainly metabolized by P450s, such as CYP3A4, CYP2C8 and CYP2C9, in the liver, and the TBF-A will covalently bind to hepatic protein and/or concentrate in the bile. Studies on metabolism-mediated immune responses will be our future subjects.

The activation of MAP kinases such as ERK1/2, p38 MAP kinase, and JNK1/2 is important in mediating many macrophage functions, including the activation of various transcription factors and the production of pro-inflammatory cytokines (Payne et al. 1991; DeFranco et al. 1998). In this study, terbinafine activated ERK1/2 and p38 MAP kinase pathways in THP-1 cells (Fig. 4). To determine the involvement of MAP kinases in transcriptional and translational regulation of terbinafine-induced IL-8 and TNFα release, blocking studies were performed using specific inhibitors of MAP kinases, including U0126, SB203580, and SP600125 (English and Cobb 2002). The mRNA expression levels and the release of IL-8 and TNFα increased by terbinafine were significantly suppressed by the pretreatment by U0126 but not by SB203580 (Fig. 5). These results suggested that an ERK pathway is mainly involved in IL-8 and TNFα release from THP-1 cells at the transcriptional level. In addition, the increase of IL-8 and TNFα in THP-1 cells was enhanced by the pretreatment with SB203580 (Fig. 5). It was demonstrated that SB203580 activated members of the ERK cascade, c-Raf, MEK, and ERK, in THP-1 cells. The activation of these kinases was sustained for at least 24 h after SB203580 treatment (Ishii et al. 2001; Numazawa et al. 2003). SB203580 activates the ERK cascades without transducing the signal into the nucleus. When cells are treated with stimulants, such as drugs, the impaired ERK signal transduction caused by the inhibitor may turn over and lead to synergistic enhancement of ERK cascade-dependent gene expression (Numazawa et al. 2003). Thus, care should be taken when applying P38 MAP kinase inhibitors to evaluate the inflammation reactions. THP-1 cells also have been reported to show enhance of ERK cascade by SB202190 (another p38 MAP kinase inhibitor), resulting in the increase of cell growth (Hirosawa et al. 2009). In this study, we confirmed that the effects of SB202190 in this study were the same as those of SB203580 (data not shown). Considering these reports, the increase of IL-8 and TNFα levels in THP-1 cells by SB203580 would be due to the activation of an ERK pathway.

Conclusion

In this study, we found that terbinafine stimulates human monocytic THP-1 cells resulting in IL-8 and TNFα release. It is suggested that terbinafine increases the pro-inflammatory cytokine release from monocytes and macrophages and activates the inflammatory response, which might result in immune-mediated hepatic injury. The findings presented here provide important insight concerning terbinafine-induced liver injury.

Conflict of interest statement

The authors declare that there are no conflicts of interest.

Acknowledgements

We thank Mr. Brent Bell for reviewing the manuscript. This work was supported by Health and Labor Sciences Research Grants from the Ministry of Health, Labor, and Welfare of Japan (H20-BIO-G001).

References

Baggiolini M, Dewald B, Moser B. Interleukin-8 and related chemotactic cytokines-CXC and CC chemokines. Advances in Immunology 55, 97–179, 1994.

Bradham CA, Plümpe J, Manns MP, Brenner DA, Trautwein C. Mechanisms of hepatic toxicity. I. TNF-induced liver injury. American Journal of Physiology. Gastrointestinal and Liver Physiology 275 (3), 387–392, 1998.

Chang CH, Young-Xu Y, Kurth T, Orav JE, Chan AK. The safety of oral antifungal treatments for superficial dermatophytosis and onychomycosis: a meta-analysis. The American Journal of Medicine 120 (9), 791–798, 2007.

DeFranco AL, Crowley MT, Finn A, Hambleton J, Weinstein SL. The role of tyrosine kinases and map kinases in LPS-induced signaling. Progress in Clinical and Biological Research 397, 119–136, 1998.

Deng X, Luyendyk JP, Ganey PE, Roth RA. Inflammatory stress and idiosyncratic hepatotoxicity: hints from animal models. Pharmacological Reviews 61 (3), 262–282, 2009.

Edling Y, Sivertsson L, Andersson TB, Porsmyr-Palmertz M, Ingelman-Sundberg M. Pro-inflammatory response and adverse drug reactions: mechanisms of action of ximelagatran on chemokine and cytokine activation in a monocyte in vitro model. Toxicology In Vitro 22 (6), 1588–1594, 2008.

Edling Y, Sivertsson LK, Butura A, Ingelman-Sundberg M, Ek M. Increased sensitivity for troglitazone-induced cytotoxicity using a human in vitro co-culture model. Toxicology In Vitro 23 (7), 1387–1395, 2009.

English JM, Cobb MH. Pharmacological inhibitors of MAPK pathways. Trends in Pharmacolical Sciences 23 (1), 40–45, 2002.

Fernandes NF, Geller SA, Fong TL. Terbinafine hepatotoxicity: case report and review of the literature. The American Journal of Gastroenterology 93 (3), 459–460, 1998.

Ganey PE, Luyendyk JP, Maddox JF, Roth RA. Adverse hepatic drug reactions: inflammatory episodes as consequence and contributor. Chemico-Biological Interactions 150 (1), 35–51, 2004.

García Rodríguez LA, Duque A, Castellsague J, Pérez-Gutthann S, Stricker BH. A cohort study on the risk of acute liver injury among users of ketoconazole and other antifungal drugs. British Journal of Clinical Pharmacology 48 (6), 847–852, 1999.

Gupta AK, Porges AJ. Hypersensitivity syndrome reaction to oral terbinafine. Australas. Journal of Dermatology 39 (3), 171–172, 1998.

Gupta AK, Shear NH. Terbinafine: an update. Journal of The American Academy of Dermatology 37 (6), 979–988, 1997.

Gupta AK, Kopstein JB, Shear NH. Hypersensitivity reaction to terbinafine. Journal of the American Academy of Dermatology 36 (6), 1018–1019, 1997.

Hall M, Monka C, Krupp P, O'Sullivan D. Safety of oral terbinafine: results of a postmarketing surveillance study in 25, 884 patients. Archives of Dermatology 133 (10), 1213–1219, 1997.

Hirosawa M, Nakahara M, Otosaka R, Imoto A, Okazaki T, Takahashi S. The p38 pathway inhibitor SB202190 activates MEK/MAPK to stimulate the growth of leukemia cells. Leukemia Research 33 (5), 693–699, 2009.

Ishii Y, Sakai S, Honma Y. Pyridinyl imidazole inhibitor SB203580 activates p44/42 mitogen-activated protein kinase and induces the differentiation of human myeloid leukemia cells. Leukemia Research 25 (9), 813–820, 2001.

Iverson SL, Uetrecht JP. Identificaion of a reactive metabolite ot terbinafine: Insights into terbinafine-induced hepatotocity. Chemical Research in Toxcicology 14 (2), 175–181, 2001.

Jaeschke H. Role of inflammation in the mechanism of acetaminophen-induced hepatotoxicity. Expert Opinion on Drug Metabolism & Toxicology 1 (3), 389–397, 2005.

Kovarik JM, Kirkesseli S, Humbert H, Grass P, Kutz K. Dose proportional pharmacokinetics of terbinafine and its N-demethylated metabolite in healthy volunteers. The British Journal of Dermatology 126 (Suppl 39), 8–13, 1992.

Laemmli UK. Cleavage of structural proteins during the assembly of the head of bacteriophage T4. Nature 227 (5289), 680–685, 1970.

Leonard EJ, Yoshimura T, Tanaka S, Raffeld M. Neutrophil recruitment by intradermally injected neutrophil attractant/activation protein-1. The Journal of Investigative Dermatology 96 (5), 690–694, 1991.

Mallat A, Zafrani ES, Metreau JM, Dhumeaux D. Terbinafine-induced prolonged cholestasis with reduction of interlobular bile ducts. Digestive Diseases and Sciences 42 (7), 1486–1488, 1997.

Numazawa S, Watabe M, Nishimura S, Kurosawa M, Izuno M, Yoshida T. Regulation of ERK-mediated signal transduction by p38 MAP kinase in human monocytic THP-1 cells. Journal of Biochemstry 133 (5), 599–605, 2003.

Payne DM, Rossomando AJ, Martino P, Erickson AK, Her JH, Shabanowitz J, Hunt DF, Weber MJ, Sturgill TW. Identification of the regulatory phosphorylation sites in pp 42/mitogen-activated protein kinase (MAP kinase). The EMBO Journal 10 (4), 885–892, 1991.

Roth RA, Luyendyk JP, Maddox JF, Ganey PE. Inflammation and drug idiosyncrasy—is there a connection? Journal of Pharmacology and Experimental Therapeutics 307 (1), 1–8, 2003.

Tafazoli S, Spehar DD, O'Brien PJ. Oxidative stress mediated idiosyncratic drug toxicity. Drug Metabolism Reviews 37 (2), 311–325, 2005.

Teobald I, Dunnion DJ, Whitbread M, Curnow SJ, Browning MJ. Phenotypic and functional differentiation of KG-1 into dendritic-like cells. Immunobiology 213 (1), 75–86, 2008.

Uetrecht JP. New concepts in immunology relevant to idiosyncratic drug reactions: the "danger hypothesis" and innate immune system. Chemical Research in Toxicology 12 (5), 387–395, 1999.

van't Wout JW, Herrmann WA, de Vries RA, Stricker BH. Terbinafine-associated hepatic injury. Journal of Hepatology 21 (1), 115–117, 1994.

Zapata Garrido AJ, Romo AC, Padilla FB. Terbinafine hepatotoxicity. A case report and review of literature. Annals of Hepatology 2 (1), 47–51, 2003.

Arch Toxicol (2011) 85:199–207
DOI 10.1007/s00204-010-0584-y

MOLECULAR TOXICOLOGY

Stimulation of pro-inflammatory responses by mebendazole in human monocytic THP-1 cells through an ERK signaling pathway

Katsuhiko Mizuno · Yasuyuki Toyoda · Tatsuki Fukami · Miki Nakajima · Tsuyoshi Yokoi

Received: 8 June 2010 / Accepted: 1 September 2010 / Published online: 17 September 2010

Abstract Oral helminthic mebendazole (MBZ) has been reported to cause liver injury with inflammatory responses. However, the underlying mechanism remains unknown. To examine the inflammatory reactions, we investigated whether MBZ and other helminthic drugs increase the release of pro-inflammatory cytokines and chemokines using human monocytic cells. The release of interleukin (IL)-8 and tumor necrosis factor (TNF) α from human monocytic THP-1 cells was significantly increased by treatment with MBZ, albendazole (ABZ), fenbendazole (FBZ), or oxibendazole (OBZ), but not by albendazole sulfoxide or praziquantel, suggesting that MBZ and structurally similar drugs can stimulate monocytes and increase the release of pro-inflammatory cytokines. MBZ also significantly increased the phosphorylation of extracellular signal-regulated kinase (ERK) 1/2 and c-Jun N-terminal kinase (JNK) 1/2 in THP-1 cells. Pretreatment with the MAP kinase/ERK kinase 1/2 inhibitor U0126 significantly suppressed the increase of IL-8 and TNFα levels by MBZ, ABZ, FBZ, or OBZ treatment in THP-1 cells, but the p38 mitogen-activated protein kinase inhibitor SB203580 or JNK1/2 inhibitor SP600125 did not. These results suggested that an ERK1/2 pathway plays an important role in the release of IL-8 and TNFα in THP-1 cells treated with MBZ and structurally similar drugs. In conclusion, the release of inflammatory mediators by MBZ might be one of the mechanisms underlying immune-mediated liver injury. This in vitro method may be useful to predict adverse inflammatory reactions that lead to hepatotoxicity.

Keywords Mebendazole · THP-1 cell · Hepatotoxicity · IL-8 · TNFα

K. Mizuno · Y. Toyoda · T. Fukami · M. Nakajima · T. Yokoi (✉)
Drug Metabolism and Toxicology, Faculty of Pharmaceutical Sciences, Kanazawa University, Kakuma-machi, Kanazawa 920-1192, Japan
e-mail: tyokoi@kenroku.kanazawa-u.ac.jp

Introduction

Drug-induced liver injury is the most frequent reason for the withdrawal of an approved drug from the market and for failures in drug development in pharmaceutical companies. Because of significant adverse drug reactions associated with hepatotoxicity, several drugs have been removed from the pharmaceutical market (Holt and Ju, 2006). Inflammatory stress might be caused by xenobiotics or drugs leading to idiosyncratic adverse drug reactions. The sporadic occurrence of acute inflammatory episodes could explain the onset of some idiosyncratic reactions during clinical drug therapy (Ganey et al. 2004; Roth et al. 2003; Tafazoli et al. 2005). Inflammatory reactions in liver are induced by the activation of immune cells, such as monocytes, macrophages and Kupffer cells. Activated monocytes and macrophages release large amounts of pro-inflammatory cytokines and chemokines, including interleukin (IL)-1, tumor necrosis factor (TNF) α, and IL-8. TNFα triggers the release of a cascade of other cytokines and recruits activated immune cells, including lymphocytes and macrophages (Bradham et al. 1998). IL-8 exhibits multiple effects on neutrophils, including the induction of lysosomal enzyme release, the increase in the expression of adhesion molecules, and rapid infiltration (Leonard et al. 1991; Baggiolini et al. 1994). In several rodent models, it was shown that the production of TNFα and neurtophil infiltration in liver play a critical role in immune-mediated

liver injury by drugs such as acetaminophen, non-steroidal anti-inflammatory drugs, and antibiotics (Jaeschke 2005; Deng et al. 2009).

Recently, it has been reported that human monocytic cell lines were useful to examine the inflammatory responses mediated by drugs withdrawn from the market. In human monocytic THP-1 cells, the mRNA expression levels and/or the release of pro-inflammatory cytokines and chemokines were increased by the treatment with troglitazone or ximelagatran (Edling et al. 2008, 2009).

Many benzimidazoles have been launched on the market and used in clinical drug therapy. Mebendazole (MBZ) and other structurally related drugs are used for the therapy of various helminthic infections as well as for the treatment of hydatid disease and alveolar echinococcosis (Ammann and Eckert 1996). However, MBZ has been reported to cause hepatic injury. Bekhti and Pirotte (1987) described a case of acute hepatocellular injury in a patient treated with MBZ 600 mg/day for echinococcosis. Colle et al. (1999) reported a case of granulomatous hepatitis with eosinophilia after the administration of MBZ. Seitz et al. (1983) and Junge and Mohr (1983) reported MBZ-induced hepatic injury, and the liver biopsy of the patient revealed hepatocytic necrosis and portal inflammation with eosinophils during long-term (49–60 days) and high-dose (2–3.5 g/day) therapy with MBZ. Recently, MBZ has been carefully used in clinical drug therapy, thus case reports of severe hepatic injury are very rare (Bagheri et al. 2004). Chen et al. (2003) reported that MBZ is associated with Steven-Johnson syndrome (SJS)/toxic epidermal necrolysis (TEN), suggesting the involvement of immune-mediated factors. However, the mechanism underlying the hepatic injury by MBZ remains to be clarified.

Considering the case reports of hepatic injury by MBZ, we hypothesized that benzimidazoles stimulate inflammatory responses that may result in immune-mediated hepatic injury. The purpose of this study is to investigate whether benzimidazoles stimulate the release of pro-inflammatory cytokines and chemokines from human monocytic cells and to clarify the involvement of cell signaling in the release of pro-inflammatory cytokines and chemokines from THP-1 cells.

Materials and methods

Materials

ABZ, fenbendazole (FBZ), MBZ, oxibendazole (OBZ), and praziquantel (PZQ) were purchased from Sigma–Aldrich (St. Louis, MO). Albendazole sulfoxide (ABZSO) was purchased from Toronto Reserch Chemicals (Ontario, Canada). Lipopolysaccharide (LPS) was also from Sigma–Aldrich (St. Louis, MO). Primers were commercially synthesized at Hokkaido System Sciences (Sapporo, Japan). The monoclonal antibodies of anti-Thr202/Tyr204 phosphorylated extracellular signal-regulated kinase (ERK) 1/2, anti-Thr180/Tyr182 phosphorylated p38 mitogen-activated protein (MAP) kinase, and anti-Thr183/Tyr185 phosphorylated c-Jun N-terminal kinase (JNK) 1/2 were purchased from Cell Signaling Technology (Beverly, MA). The monoclonal antibodies against ERK1/2 and JNK1/2 and the polyclonal antibody against p38 MAP kinase were also from Cell Signaling Technology. All other reagents were of the highest grade commercially available.

Cell culture

The human monocytic leukemia cell line THP-1 was obtained from Riken Gene Bank (Tsukuba, Japan). HL-60 and KG-1 cells were obtained from American Type Culture Collection (Manassas, VA). THP-1 cells were cultured in RPMI 1640 medium (Nissui Pharmaceutical, Tokyo, Japan) supplemented with 10% fetal bovine serum (FBS; Invitrogen, Carlsbad, CA). HL-60 and KG-1 cells were cultured in RPMI 1640 medium supplemented with 20% FBS. These cells were maintained at 37°C under an atmosphere of 5% CO_2.

Drug treatment of human monocytic cell lines

THP-1, HL-60, and KG-1 cells were seeded at a density of 1×10^6 cells/well in 24-well plates with the medium containing the indicated concentration of helminthic drugs, and then incubated at 37°C. The final concentration of dimethyl sulfoxide (DMSO) in medium was 0.1%. In experiments using MAP kinase inhibitors, cells were pretreated with MAP kinase/ERK kinase (MEK) 1/2 inhibitor U0126 (Wako Pure Chemical Industries), p38 MAP kinase inhibitor SB203580 (Wako Pure Chemical Industries), or JNK1/2 inhibitor SP600125 (Calbiochem, Los Angeles, CA) for 1 h, and then treated with the helminthic drugs. Supernatants were separated from cell cultures by centrifugation and stored at −70°C until assayed. For immunoblot analysis, the cells were suspended in TGE buffer (10 mM Tris–HCl, 20% glycerol, 1 mM EDTA, pH 7.4) and disrupted by freeze-thawing three times.

Enzyme-linked immunosorbent assay (ELISA)

The pro-inflammatory cytokine TNFα and the chemokine IL-8 in cell supernatants were measured by Human TNFα and IL-8 ELISA Ready-SET-GO!™ (eBioscience, San Diego, CA) according to the manufacturer's instructions.

Real-time reverse transcription-polymerase chain reaction (RT–PCR)

Total RNA was extracted from THP-1 cells with RNAiso (Takara Bio, Shiga, Japan) according to the protocol supplied by the manufacturer. Reverse transcription was performed with ReverTra Ace (Toyobo, Tokyo, Japan) according to the manufacturer's protocol. For quantitative analysis, real-time RT–PCR was performed for inflammatory cytokine mRNA using an MX3000P real-time PCR system (Stratagene, La Jolla, CA). The primers used in this study were human IL-8 (forward: 5′-CAGCCTTCCTG ATTTCTCTGCAG-3′, reverse: 5′-AGACAGAGCTCTC TTCCATCAG-3′) and human TNFα (forward: 5′-CTT CTGCCTGCTGCACTTTGGAG-3′, reverse: 5′-GGCTAC AGGCTTGTCACTCGG-3′). An 1 μL portion of the reverse-transcribed mixture was added to a PCR mixture containing 10 pmol of each primer and 10 μL of SYBR Premix ExTaq solution in a final volume of 20 μL. After an initial denaturation at 95°C for 30 s, the amplification was performed by denaturation at 94°C for 20 s and annealing and extension at 64°C for 20 s for 45 cycles. The IL-8 and TNFα mRNA levels were normalized with human glyceraldehyde 3-phosphate dehydrogenase (GAPDH) mRNA (forward: 5′-CCATGAGAAGTATGACAACAGCC-3′, 5′-TG GGTGGCAGTGATGGCATGGA-3′).

Immunoblot analysis

SDS–polyacrylamide gel electrophoresis and immunoblot analysis were performed according to Laemmli (1970). Cell sources (25 μg) were separated on 10% polyacrylamide gels and electrotransferred onto polyvinylidene difluoride membrane, Immobilon-P (Millipore Corporation, Billerica, MA). The membranes were probed with the monoclonal antibodies of anti-Thr202/Tyr204 phosphorylated ERK1/2, anti-Thr180/Tyr182 phosphorylated p38 MAP kinase, and anti-Thr183/Tyr185 phosphorylated JNK1/2, and the corresponding fluorescent dye-conjugated second antibody and an Odyssey Infrared Imaging system (LI-COR Biosciences, Lincoln, NE) were used for the detection. The relative expression level was quantified using ImageQuant TL Image Analysis software (GE Healthcare, Little Chalfont, Buckinghamshire, UK).

Cell viability assay

For the cell viability assay, THP-1 cells were seeded at a density of 1×10^5 cells/well in 96-well plates with the medium containing the indicated concentration of the halminthic drug, and then incubated at 37°C. The final concentration of DMSO in medium was 0.1%. After 6 or 24 h incubation, cell viability was evaluated by 3-(4,5-dimetylthiazol-2-yl)-2, 5-diphenyl tetrazolium bromide (MTT) activities using a CellTiter-Blue Cell Viability Assay (Promega, Medison, WI) according to the manufacturer's protocol. The fluorescence of the generated resorufin was detected fluorometrically (excitation: 338 nm, emission: 458 nm) by using a luminometer (1420 ARVO MX, Wallac, Turku, Finland).

Statistical analysis

Data are expressed as mean ± SD of triplicate determinations. Comparison of 2 groups was made with an unpaired, two-tailed student's *t*-test. Comparison of multiple groups was made with ANOVA followed by Dunnett or Tukey test. A value of $P < 0.05$ was considered statistically significant.

Results

Comparative effect of helminthic drugs on human monocytic cell lines

To investigate whether the helminthic drugs increased the release of IL-8 and TNFα from human monocytic cells, cells were treated with 10 μM of the helminthic drugs for 6 h and then the release of IL-8 and TNFα in the cell supernatants was measured by ELISA. The helminthic drugs used in our study are shown in Fig. 1. ABZSO was the active metabolite of ABZ (Gottschall et al. 1990). FBZ and OBZ were used as drugs structurally similar to MBZ and ABZ, although they have never been administered in humans. PZQ was used because no case of symptomatic hepatic injury has ever been seen so far. The IL-8 and TNFα release from THP-1 cells was significantly increased by treatment with ABZ, FBZ, MBZ, or OBZ but not by ABZSO or PZQ compared with control (0.1% DMSO) (Fig. 2a, b). These results suggested that MBZ and structurally similar drugs have the ability to increase the release of pro-inflammatory cytokines and chemokines from monocytes that activate the inflammatory responses. In addition, MBZ and OBZ also significantly increased the IL-8 release from HL-60 and KG-1 cells and FBZ significantly increased the IL-8 release from KG-1 cells (Fig. 2c, e). In contrast, the TNFα release from HL-60 and KG-1 cells was not increased by these helminthic drugs (Fig. 2d, f). For the subsequent analyses, THP-1 cells were used because they showed the highest sensitivity for the release.

Time-dependent changes in the mRNA expression levels and the release of IL-8 and TNFα in THP-1 cells treated with MBZ

We next investigated the time-dependent changes of the IL-8 and TNFα levels in THP-1 cells. By the treatment

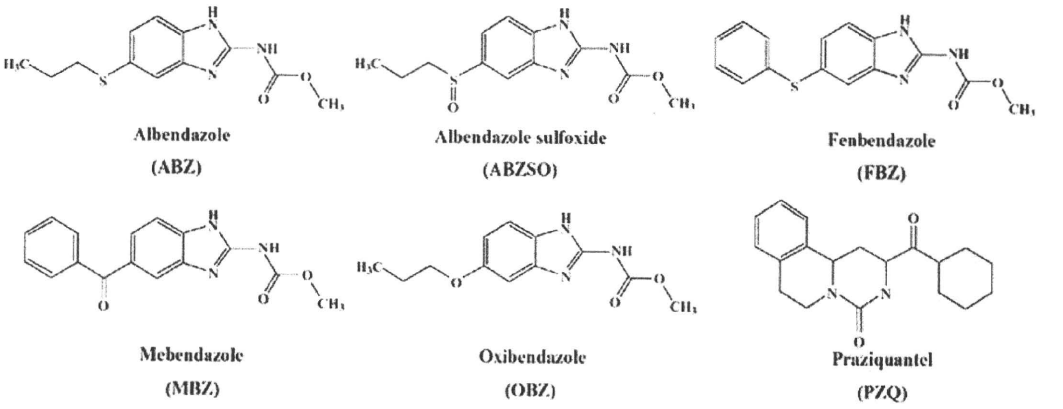

Fig. 1 Chemical structures of the helminthic drugs used in the present study

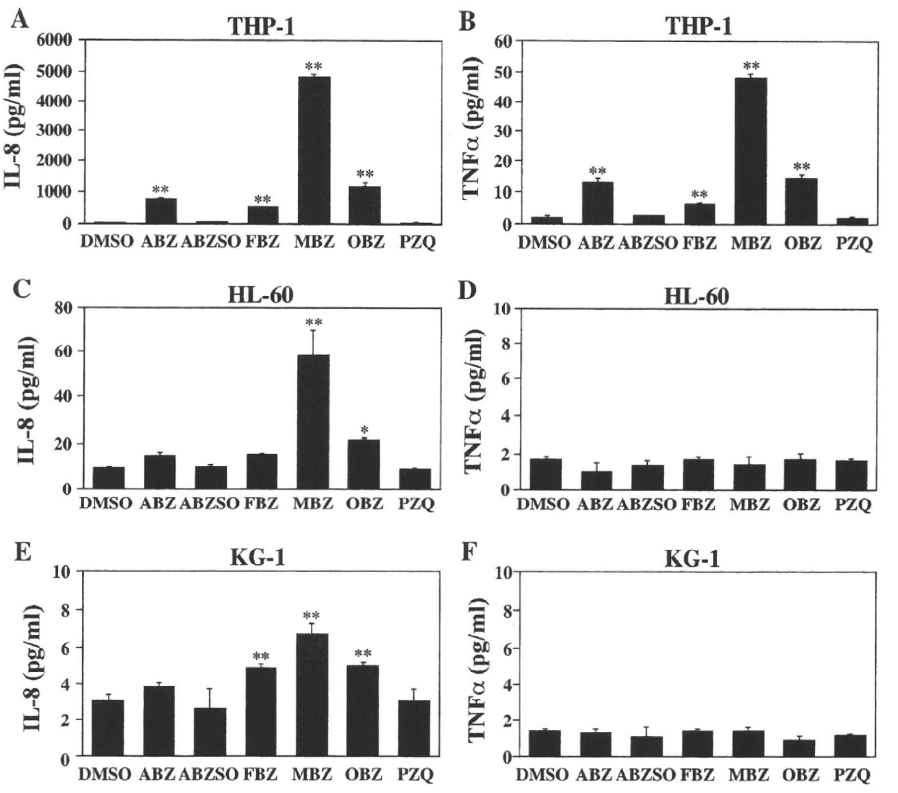

Fig. 2 Effects of helminthic drugs on the release of IL-8 and TNFα from human monocytic cell lines. Human monocytic cell lines including THP-1 (**a** and **b**), HL-60 (**c** and **d**), and KG-1 (**e** and **f**) were treated with 10 μM of the helminthic drugs for 6 h. The release of IL-8 (**a**, **c**, and **e**) and TNFα (**b**, **d**, and **f**) in the supernatant was measured by ELISA. Data represent the mean ± SD of triplicate determinations. $*P < 0.05$; $**P < 0.01$, compared with control (0.1% DMSO)

with 10 μM MBZ, the mRNA expression levels and the release of IL-8 and TNFα in THP-1 cells were significantly increased for 1.5–24 h compared with control (Fig. 3). The mRNA expression levels of IL-8 were mostly increased at 6 h incubation but the increase of IL-8 release was in a time-dependent manner (Fig. 3a, c). The highest increase of the mRNA expression levels and the release of TNFα appeared at 4.5 and 6 h-incubation, respectively (Fig. 3b, d). Therefore, an incubation time of 6 h was selected for further assay to measure the release of IL-8 and TNFα. To investigate whether there were cytotoxic effects on THP-1 cells caused by the leakage of intercellular cytokines and chemokines, a cell viability assay for THP-1 cells was performed. At 24 h-incubation, these helminthic drugs had no cytotoxic effects on THP-1 cells (data not shown).

Dose-dependent changes in the release of IL-8 and TNFα from THP-1 cells treated with helminthic drugs

To investigate whether the helminthic drugs at a lower concentration could also lead to IL-8 and TNFα release in

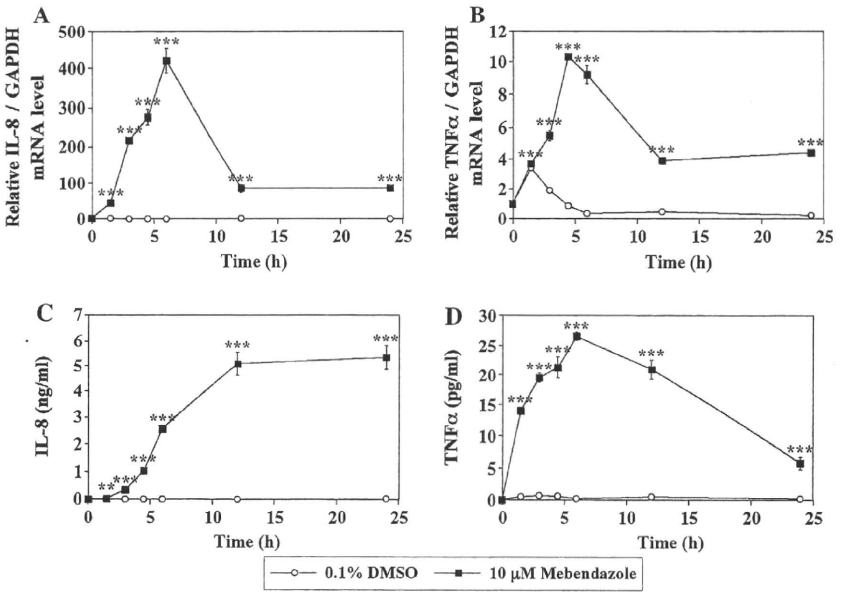

Fig. 3 Time-dependent changes in the mRNA expression levels and the release of IL-8 and TNFα in THP-1 cells treated with MBZ. THP-1 cells were treated with 10 μM MBZ for various durations. The mRNA expression levels of IL-8 (**a**) and TNFα (**b**) in THP-1 cells were measured by real-time RT–PCR analysis. The release of IL-8 (**c**) and TNFα (**d**) in the supernatant was measured by ELISA. Data represent the mean ± SD of triplicate determinations. $^{**}P < 0.01$; $^{***}P < 0.001$, compared with control (0.1% DMSO) of each time point

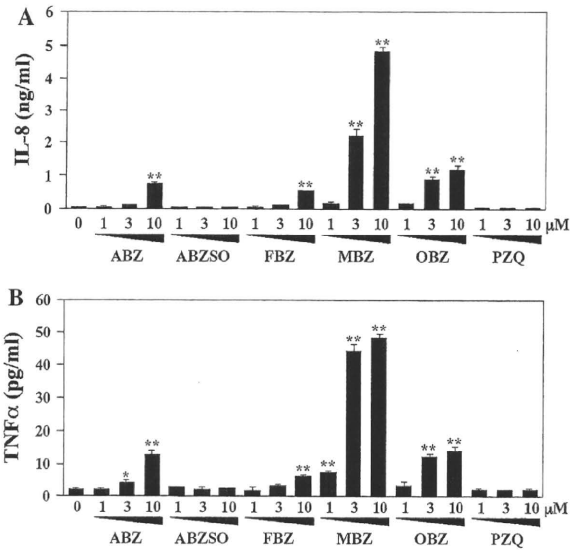

Fig. 4 Dose-dependent changes in the release of IL-8 and TNFα from THP-1 cells treated with helminthic drugs. THP-1 cells were treated with the indicated concentrations of the helminthic drugs. After incubation for 6 h, the release of IL-8 (**a**) and TNFα (**b**) in the supernatant was measured by ELISA. Data represent the mean ± SD of triplicate determinations. $^{*}P < 0.05$; $^{**}P < 0.01$, compared with control (0.1% DMSO)

THP-1 cells, THP-1 cells were treated with helminthic drugs at the indicated concentration for 6 h and then the release of IL-8 and TNFα was measured. As shown in Fig. 4, ABZ, FBZ, MBZ, and OBZ increased the IL-8 and TNFα levels in a dose-dependent manner. In addition, at least 3 μM MBZ was required to increase the release of IL-8 in THP-1 cells. In contrast, the TNFα release was significantly increased at 1 μM MBZ.

Activation of MAP kinase signaling pathway in THP-1 cells treated with MBZ

MAP kinases, including ERK1/2, p38 MAP kinase, and JNK1/2, are major components for many intracellular signaling pathways. The phosphorylation of MAP kinases, which is required for the enzyme activity, activates signaling cascades, the down stream effects of which have been linked to the regulation of the inflammatory response (DeFranco et al. 1998). To clarify the role of MAP kinase signaling pathway in the activation of THP-1 cells, the phosphorylation of ERK1/2 (44/42 kDa), p38 MAP kinase (43 kDa), and JNK1/2 (46/54 kDa) in cell lysates was assessed by immunoblot analysis. A sample treated with 2 μg/ml LPS was used as a positive control for the phosphorylation of MAP kinases. As shown in Fig. 5, MBZ treatment for 1 h significantly increased the phosphorylation of ERK1/2 and JNK1/2 but not p38 MAP kinase in THP-1 cells. These results suggested that MBZ activated ERK1/2 and JNK1/2 pathways in THP-1 cells. In addition, to confirm the effects of MAP kinase inhibitors on the phosphorylation of ERK1/2, p38 MAP kinase, and JNK1/2, THP-1 cells were pretreated for 1 h with various concentrations of MEK1/2 inhibitor U0126, p38 MAP kinase inhibitor SB203580, or JNK1/2 inhibitor SP600125 (English and Cobb, 2002) before the treatment with 10 μM MBZ. As a result, the phosphorylation of ERK1/2 was significantly suppressed by the pretreatment with the specific inhibitor U0126 but not that of JNK1/2 (Fig. 5).

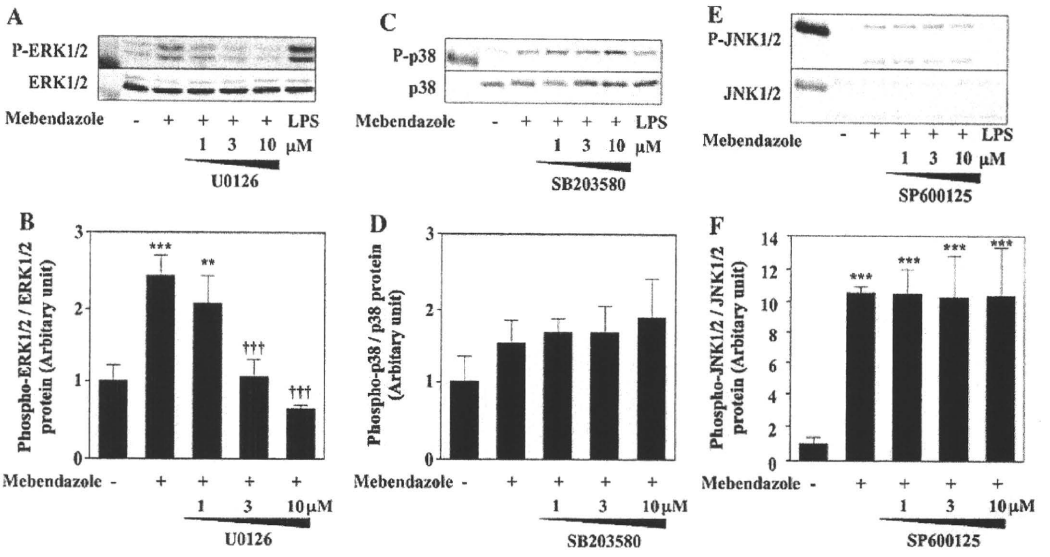

Fig. 5 Activation of MAP kinase signaling pathways in THP-1 cells treated with MBZ. Immunoblot analyses of MAP kinase proteins in THP-1 cells were performed (**a**, **c**, and **e**) and quantified (**b**, **d**, and **f**). Before the treatment with 10 μM MBZ, THP-1 cells were pretreated with the indicated concentrations of MAP kinase inhibitors for 1 h. U0126, SB203580, and, SP600125 were used as specific inhibitors of MEK1/2, p38 MAP kinase, and, JNK1/2, respectively. After 1 h-incubation with MBZ, cell lysates were subjected to immunoblot analyses using antibodies of anti-Thr202/Tyr204 phosphorylated ERK1/2 (**a** and **b**), anti-Thr180/Tyr182 phosphorylated p38 MAP kinase (**c** and **d**), and anti-Thr183/Tyr185 phosphorylated JNK1/2 (**e** and **f**). The same sample treated with 2 μg/ml LPS was used as a positive control. Data represent the mean ± SD of triplicate determinations. $^{**}P < 0.01$; $^{***}P < 0.001$, compared with control (0.1% DMSO). $\dagger\dagger P < 0.01$; $\dagger\dagger\dagger P < 0.001$, compared with MBZ only

The phosphorylation of JNK1/2 treated with LPS was suppressed by the pretreatment with the specific inhibitor SP600125 (data not shown).

Effects of MAP kinase inhibitors on the release of IL-8 and TNFα from THP-1 cells treated with helminthic drugs

To clarify which MAP kinase signaling pathway is mainly involved in the increase of IL-8 and TNFα release, the effects of MAP kinase inhibitors on the release of IL-8 and TNFα from THP-1 cells treated with MBZ were investigated. As shown in Fig. 6, the increased release of IL-8 and TNFα by MBZ treatment from THP-1 cells was significantly suppressed in a dose dependent manner by the pretreatment with U0126, suggesting that an ERK1/2 pathway plays an important role in the release of IL-8 and TNFα by MBZ treatment. A suppressing effect by SP600125 was not observed. In contrast, the increase of IL-8 and TNFα release was enhanced by the pretreatment with SB203580. Therefore, we investigated the effects of MAP kinase inhibitors on the release of IL-8 and TNFα from THP-1 cells treated with other helminthic drugs. As shown in Fig. 7, with ABZ, FBZ, or OBZ treatment, the pretreatment with U0126 remarkably suppressed the increase of IL-8 and TNFα in THP-1 cells and those of SB203580 and SP600125 had no suppressive effects. These results suggested that an ERK1/2 pathway also plays an important role in the increase of IL-8 and TNFα by ABZ, FBZ, or OBZ treatment as well as MBZ treatment. In contrast, even for the control, the basal IL-8 and TNFα levels in THP-1 cells were significantly suppressed by the pretreatment with U0126 and were increased by the pretreatment with SB203580, suggesting that the basal IL-8 and TNFα levels in THP-1 cells were affected by the MAP kinase inhibitors. In the case of ABZSO and PZQ, the effects of MAP kinase inhibitors on the IL-8 and TNFα levels in THP-1 cells were similar to those of the control (0.1% DMSO).

Discussion

For in vitro studies of the differentiation and activation of immune cells, human monocytic cell lines, THP-1, HL-60, and KG-1 cells are usually employed. In the present study, by the treatment with the helminthic drugs MBZ, IL-8 release from THP-1, HL-60, and KG-1 cells and TNFα release from THP-1 cells was significantly increased compared with the control (Fig. 2a–c, e). In the case of ABZ, FBZ, or OBZ, the release of IL-8 and TNFα from THP-1 cells was also significantly increased compared with the control (Fig. 2a, b). This suggested that MBZ and structurally similar drugs have the ability to stimulate the

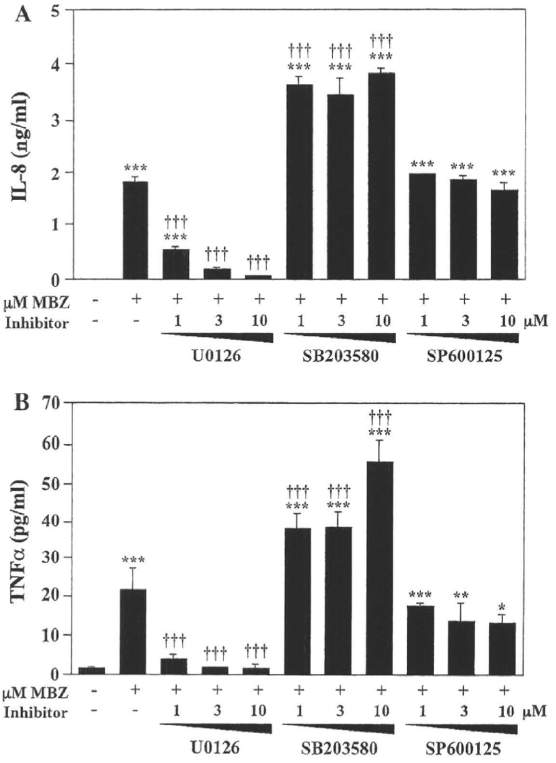

Fig. 6 Effects of MAP kinase inhibitors on the IL-8 and TNFα release from THP-1 cells treated with MBZ. Before the treatment with 10 μM MBZ, THP-1 cells were pretreated with the indicated concentrations of MAP kinase inhibitors for 1 h. After 6 h-incubation with MBZ, the release of IL-8 (**a**) and TNFα (**b**) in the supernatant was measured by ELISA. Data represent the mean ± SD of triplicate determinations. $*P < 0.05$; $**P < 0.01$; $***P < 0.001$, compared with control (0.1% DMSO). $\dagger P < 0.05$; $\dagger\dagger P < 0.01$; $\dagger\dagger\dagger P < 0.001$, compared with MBZ only

release of pro-inflammatory cytokines from monocytes, leading to the activation of the inflammatory reaction. In contrast, PZQ, used as a negative control for MBZ, had no effects on the cytokine release in human monocytic cells. This result was supported by the fact that no case of symptomatic hepatic injury has ever been seen so far.

We found that MBZ stimulates the release of pro-inflammatory cytokines and chemokines from human monocytic cells. The activation of inflammatory responses might be one of the mechanisms underlying the immune-mediated liver injury by MBZ. On the other hand, the activation of human monocytic cells by other drugs, such as ximelagatran and troglitazone, has been reported recently, although these drugs have already been withdrawn from the market due to idiosyncratic hepatic injury (Edling et al. 2008, 2009). Ximelagatran increased the release of chemokines from THP-1 cells but the types of released cytokines and the time dependent change of the cytokine release by the drug treatment were different from the case of MBZ (Edling et al. 2008). In addition, troglitazone increased the mRNA expression levels of pro-inflammatory cytokines and chemokines in THP-1 cells (Edling et al. 2009). Therefore, measurement of the release of pro-inflammatory cytokines and chemokines from human monocytic cells may be useful to predict the possibility of adverse reactions to drugs involving immune-mediated hepatic injury.

The activation of MAP kinases such as ERK1/2, p38 MAP kinase, and JNK1/2 is important in mediating many macrophage functions, including the activation of various transcription factors and the production of pro-inflammatory cytokines (Payne et al. 1991; DeFranco et al.

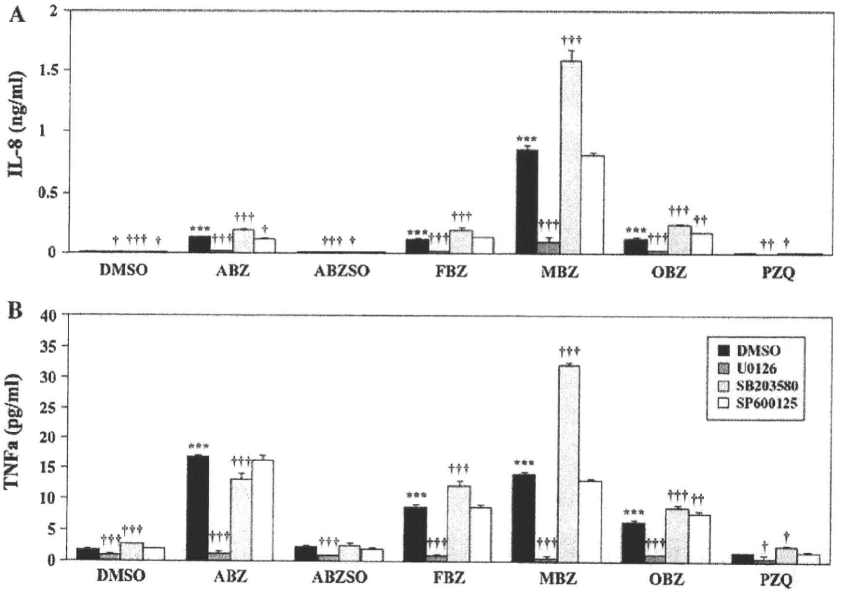

Fig. 7 Effects of MAP kinase inhibitors on the IL-8 and TNFα release from THP-1 cells treated with helminthic drugs. Before the incubation with 10 μM of the helminthic drugs, THP-1 cells were pretreated with 10 μM MAP kinase inhibitors for 1 h. After 6 h-incubation with the halminthic drugs, the release of IL-8 (**a**) and TNFα (**b**) in the supernatant was measured by ELISA. Data represent the mean ± SD of triplicate determinations. $***P < 0.001$, compared with control (0.1% DMSO). $\dagger P < 0.05$; $\dagger\dagger P < 0.01$; $\dagger\dagger\dagger P < 0.001$, compared with an helminthic drug only

1998). In this study, MBZ activated the ERK1/2 and JNK1/2 pathways in THP-1 cells (Fig. 6). Previous experiments with several MAP kinase inhibitors demonstrated that blocking MAP kinase prevents IL-8 and TNFα release from LPS-stimulated monocytes at the transcription and translation levels (Guha and Mackman 2001). To determine the involvement of MAP kinases in MBZ-induced IL-8 and TNFα release, blocking studies were performed using specific inhibitors of MAP kinases, including U0126, SB203580, and SP600125 (English and Cobb 2002). The release of IL-8 and TNFα increased by MBZ was significantly suppressed by the U0126 pretreatment (Figs. 5, 6). These results suggested that an ERK pathway is mainly involved in IL-8 and TNFα release from THP-1 cells. In addition, the increase of IL-8 and TNFα release from THP-1 cells was enhanced by the pretreatment with SB203580 (Fig. 5). At higher concentrations, the p38 MAP kinase inhibitors have been reported to increase the phosphorylation of ERK1/2 (Ishii et al. 2001; Hirosawa et al. 2009). THP-1 cells also have been reported to show enhanced ERK cascade by SB203580 (Numazawa et al. 2003). Considering these reports, the increase of IL-8 and TNFα release from THP-1 cells by SB203580 would be due to the activation of an ERK pathway.

Elevations of serum aminotransferases have been reported to occur in 9–13% of patients treated with 50–100 mg/kg/day; however, severe hepatic injury of MBZ is very rare. Seitz et al. (1983) and Junge and Mohr (1983) reported MBZ-induced hepatic injury, and liver biopsy of the patient revealed hepatocytic necrosis and portal inflammation with eosinophils during long-term (49–60 days) and high-dose (2–3.5 g/day) therapy with MBZ. Rechallenge was followed by a marked elevation of the aminotranferase levels. Liver biopsy showed hepatocytic necrosis and portal inflammation with eosinophils (Junge and Mohr 1983), suggesting an immune-mediated drug response. Colle et al. (1999) also reported a case of granulomatous (immunoallergic) hepatitis with eosinophilia after the administration of MBZ.

It has been reported that the peak plasma concentrations of MBZ was 0.12 ± 0.08 μM 2 h after a single oral administration of 1000 mg MBZ in 16 healthy volunteers (Corti et al. 2009). Because it is very difficult to predict actual drug concentration in the liver and to extrapolate from an in vitro study to the in vivo condition in humans, it is better to test the drug effects in cell-based assays at a range of concentrations up to at least 30 times the efficacious concentration as reported by O'Brien et al. (2006). Thus, we conducted with up to 10 μM of MBZ. However, further study is necessary to clarify whether oral administration of MBZ stimulates the release of pro-inflammatory cytokines and chemokines in vivo.

We obtained ABZSO, an active metabolite of ABZ, which was investigated in this study as a structurally similar drug. ABZSO would be responsible for the systemic biological activity of ABZ, whereas ABZ sulfone is pharmacologically inert (Gottschall et al. 1990). A case report of acute hepatitis caused by ABZ was recently reported by Choi et al. (2008). In evaluating the relation of ABZ and ABZSO to the cytokine release, interestingly, pro-inflammatory cytokine release was found to be increased by treatment with ABZ, but not by ABZSO treatment in human monocytic cells (Figs. 2, 7). These results suggested that ABZ is a causal drug of hepatic injury. However, the activation of THP-1 cells by MBZ was much higher than that by ABZ.

In conclusion, we found that MBZ stimulated human monocytic THP-1 cells resulting in IL-8 and TNFα release. It is suggested that MBZ increases the pro-inflammatory cytokine release from monocytes and macrophages and activates the inflammatory response, which might result in immune-mediated hepatic injury. The findings presented here provide important insight concerning MBZ-induced liver injury.

Acknowledgments We thank Mr. Brent Bell for reviewing the manuscript. This work was supported by Health and Labor Sciences Research Grants from the Ministry of Health, Labor, and Welfare of Japan (H20-BIO-G001).

References

Ammann RW, Eckert J (1996) Cestodes. Echinococcus. Gastroenterol Clin North Am 25:655–689

Baggiolini M, Dewald B, Moser B (1994) Interleukin-8 and related chemotactic cytokines-CXC and CC chemokines. Adv Immunol 55:97–179

Bagheri H, Simiand E, Montastruc JL, Magnaval JF (2004) Adverse drug reactions to anthelmintics. Ann Pharmacother 38:383–388

Bekhti A, Pirotte J (1987) Hepatotoxicity of mebendazole, Relationship with serum concentrations of the drug. Gastroenterol Clin Biol 11:701–703

Bradham CA, Plümpe J, Manns MP, Brenner DA, Trautwein C (1998) Mechanisms of hepatic toxicity. I. TNF-induced liver injury. Am J Physiol 275:G387–G392

Chen K-T, Twu S-J, Chen H-J, Lin R-S (2003) Outbreak of Steravens-Johnson syndrome/toxic epidermal necrolysis associated with mebendazole and metronidazole use among Filipino laborers in Taiwan. Am J Public Health 93:489–492

Choi GY, Yang HW, Cho SH, Kang DW, Go H, Lee WC, Lee YJ, Jung SH, Kim AN, Cha SW (2008) Acute drug-induced hepatitis caused by albendazole. J Korean Med Sci 23:903–905. doi: 10.3346/jkms.2008.23.5.903

Colle I, Naegels S, Hoorens A, Hautekeete M (1999) Granulomatous hepatitis due to mebendazole. J Clin Gastroenterol 28:44–45

Corti N, Heck A, Rentsch K, Zingg W, Jetter A, Stieger B, Pauli-Magnus C (2009) Effect of ritonavir on the pharmacokinetics of the benzimidazoles albendazole and mebendazole: an interaction study in healthy volunteers. Eur J Clin Pharmacol 65:999–1006

DeFranco AL, Crowley MT, Finn A, Hambleton J, Weinstein SL (1998) The role of tyrosine kinases and map kinases in LPS-induced signaling. Prog Clin Biol Res 397:119–136

Deng X, Luyendyk JP, Ganey PE, Roth RA (2009) Inflammatory stress and idiosyncratic hepatotoxicity: hints from animal models. Pharmacol Rev 61:262–282. doi:10.1124/pr.109.001727

Edling Y, Sivertsson L, Andersson TB, Porsmyr-Palmertz M, Ingelman-Sundberg M (2008) Pro-inflammatory response and adverse drug reactions: mechanisms of action of ximelagatran on chemokine and cytokine activation in a monocyte in vitro model. Toxicol In Vitro 22:1588–1594. doi:10.1016/j.tiv.2008.06.011

Edling Y, Sivertsson LK, Butura A, Ingelman-Sundberg M, Ek M (2009) Increased sensitivity for troglitazone-induced cytotoxicity using a human in vitro co-culture model. Toxicol In Vitro 23:1387–1395. doi:10.1016/j.tiv.2009.07.026

English JM, Cobb MH (2002) Pharmacological inhibitors of MAPK pathways. Trends Pharmacol Sci 23:40–45

Ganey PE, Luyendyk JP, Maddox JF, Roth RA (2004) Adverse hepatic drug reactions: inflammatory episodes as consequence and contributor. Chem Biol Interact 150:35–51. doi:10.1016/j.cbi.2004.09.002

Gottschall DW, Theodorides VJ, Wang R (1990) The metabolism of benzimidazole anthelmintics. Parasitol Today 6:115–124

Guha M, Mackman N (2001) LPS induction of gene expression in human monocytes. Cell Signal 13:85–94

Hirosawa M, Nakahara M, Otosaka R, Imoto A, Okazaki T, Takahashi S (2009) The p38 pathway inhibitor SB202190 activates MEK/MAPK to stimulate the growth of leukemia cells. Leuk Res 33:693–699. doi:10.1016/j.leukres.2008.09.028

Holt MP, Ju C (2006) Mechanisms of drug-induced liver injury. AAPS J 8:E48–E54. doi:10.1208/aapsj080106

Ishii Y, Sakai S, Honma Y (2001) Pyridinyl imidazole inhibitor SB203580 activates p44/42 mitogen-activated protein kinase and induces the differentiation of human myeloid leukemia cells. Leuk Res 25:813–820

Jaeschke H (2005) Role of inflammation in the mechanism of acetaminophen-induced hepatotoxicity. Expert Opin Drug Metab Toxicol 1:389–397. doi:10.1517/17425255.1.3.389

Junge U, Mohr W (1983) Mebendazole-hepatitis. Z Gastroenterol 21:736–738

Laemmli UK (1970) Cleavage of structural proteins during the assembly of the head of bacteriophage T4. Nature 227:680–685

Leonard EJ, Yoshimura T, Tanaka S, Raffeld M (1991) Neutrophil recruitment by intradermally injected neutrophil attractant/activation protein-1. J Invest Dermatol 96:690–694

Numazawa S, Watabe M, Nishimura S, Kurosawa M, Izuno M, Yoshida T (2003) Regulation of ERK-mediated signal transduction by p38 MAP kinase in human monocytic THP-1 cells. J Biochem 133:599–605

O'Brien PJ, Irwin W, Diaz D, Howard-Cofield E, Krejsa CM, Slaughter MR, Gao B, Kaludercic N, Angeline A, Bernardi P, Brain P, Hougham C (2006) High concordance of drug-induced human hepatotoxicity with in vitro cytotoxicity measured in a novel cell-based model using high content screening. Arch Toxicol 80:580–604

Payne DM, Rossomando AJ, Martino P, Erickson AK, Her JH, Shabanowitz J, Hunt DF, Weber MJ, Sturgill TW (1991) Identification of the regulatory phosphorylation sites in pp42/mitogen-activated protein kinase (MAP kinase). EMBO J 10:885–892

Roth RA, Luyendyk JP, Maddox JF, Ganey PE (2003) Inflammation and drug idiosyncrasy-is there a connection? J Pharmacol Exp Ther 307:1–8. doi:10.1124/jpet.102.041624

Seitz R, Schwerk W, Arnold R (1983) Hepatocellular drug reactions caused by mebendazole therapy in cystic echinococcosis. Z Gastroenterol 21:324–329

Tafazoli S, Spehar DD, O'Brien PJ (2005) Oxidative stress mediated idiosyncratic drug toxicity. Drug Metab Rev 37:311–325. doi:10.1081/DMR-55227

Biochemical Pharmacology 79 (2010) 288–295

Contents lists available at ScienceDirect

Biochemical Pharmacology

journal homepage: www.elsevier.com/locate/biochempharm

Transcriptional regulation of human carboxylesterase 1A1 by nuclear factor-erythroid 2 related factor 2 (Nrf2)☆

Taiga Maruichi, Tatsuki Fukami, Miki Nakajima, Tsuyoshi Yokoi *

Drug Metabolism and Toxicology, Faculty of Pharmaceutical Sciences, Kanazawa University, Kakuma-machi, Kanazawa 920-1192, Japan

ARTICLE INFO

Article history:
Received 21 July 2009
Accepted 19 August 2009

Keywords:
Carboxylesterase
Gene regulation
Nuclear factor-erythroid 2 related factor 2

ABSTRACT

Human carboxylesterase (CES) 1A, which is predominantly expressed in liver and lung, plays an important role in the hydrolysis of endogenous compounds and xenobiotics. CES1A is reported to be induced in human hepatocytes by butylated hydroxyanisole, ticlopidine and diclofenac, and the induction is assumed to be caused by oxidative stress. However, the molecular mechanism remains to be determined. In this study, we sought to investigate whether CES1A is regulated by nuclear factor-erythroid 2 related factor 2 (Nrf2), which is a transcriptional factor activated by oxidative stress, and clarify the molecular mechanism. Real-time reverse transcription-PCR assays revealed that CES1A1 mRNA was significantly induced by *tert*-butylhydroquinone (tBHQ) and sulforaphane (SFN), which are representative activators of Nrf2 in HepG2, Caco-2 and HeLa cells. The induction was completely suppressed with small interfering RNA for Nrf2. In HepG2 cells, the CES1A protein level and imidapril hydrolase activity, which is specifically catalyzed by CES1A, were also significantly induced by tBHQ and SFN. Luciferase assays revealed that the antioxidant response element (ARE) at −2025 in the *CES1A1* gene was responsible for the transactivation by Nrf2. In addition, electrophoretic mobility shift assays and chromatin immunoprecipitation assays revealed that Nrf2 binds to the ARE in the *CES1A1* gene. These findings clearly demonstrated that human CES1A1 is induced by Nrf2. This is the first study to demonstrate the molecular mechanism of the inducible regulation of human CES1A1.

1. Introduction

Human carboxylesterase (CES) is a member of serine hydrolase superfamily and involved in the hydrolysis of endogenous compounds and xenobiotics. In human, the CES1A and CES2 families play important roles in drug metabolism. The CES1A mainly hydrolyzes substrates with a small alcohol group and large acyl group, such as imidapril [1] and osertamivir [2]. In contrast, the CES2 prefers substrates with a large alcohol group and small acyl group, such as CPT-11 [3] and heroin [4]. Since CES1A has been reported to play roles as triglyceride hydrolase (TGH) [5], acyl coenzyme A:cholesterol acyltransferase (ACAT) [6] and cholesteryl ester hydrolase (CEH) [7], it seems probable that CES1A is important for the lipid metabolism as well as the drug metabolism. CES1A is predominantly expressed in liver and lung, whereas CES2 is expressed in colon and liver [8]. Human CES1A is classified into two isoforms, CES1A1 and CES1A2, with high homology at the mRNA level (99.3%). It has been accepted that the *CES1A2* gene is inverted and duplicated with the *CES1A1* gene [9]. However, we recently demonstrated that the *CES1A2* gene is a variant of the *CES1A3* pseudogene [10]. The sequence identity in the 5′-flanking region between the *CES1A1* and *CES1A2* genes is approximately 90% and the sequences downstream intron 1 of them are identical. Since only the N-terminal signal peptide sequences in exon 1 of CES1A1 and CES1A2 are different, mature proteins produced from both mRNA are identical. Our previous study revealed that the levels of CES1A1 mRNA transcribed from the *CES1A1* gene were substantially higher in liver than those of CES1A2 mRNA transcribed from the *CES1A2* gene [10]. Therefore, it is plausible that the level of CES1A1 mRNA rather than that of CES1A2 mRNA affects the level of mature protein and enzyme activity.

Cells are protected against oxidative stress by increasing the transcription of a group of genes coding antioxidant proteins and phase II enzymes, such as NAD(P)H:quinone oxidoreductase1 (NQO1) [11], heme oxigenase1 (HO-1) [12], and UDP-glucuronosyltransferase (UGT) 1A1 [13]. The most important regulator of the up-regulation is the transcription factor nuclear factor-erythroid 2 (NF-E2) related factor 2 (Nrf2). Nrf2 is a member of the cap'n'collar (CNC) family of transcriptional factors and contains a C-terminal basic leucine zipper structure that facilitates dimerization and DNA binding [14]. Nrf2 is highly expressed in detoxification tissues such as liver and kidney, and tissues that are exposed to the

☆ This study was supported by a Grant-in-Aid for Encouragement of Young Scientists of the Ministry of Education, Science, Sports and Culture #21790148.

* Corresponding author. Tel.: +81 76 234 4407; fax: +81 76 234 4407.
E-mail address: tyokoi@kenroku.kanazawa-u.ac.jp (T. Yokoi).

0006-2952/$ – see front matter © 2009 Elsevier Inc. All rights reserved.
doi:10.1016/j.bcp.2009.08.019

external environment, such as skin, lung and gastrointestinal tract [15]. In the absence of cellular stress, Nrf2 is localized in cytosol by binding with Kelch-like erythroid cell-derived protein with CNC homology (ECH)-associated protein 1 (Keap1), which acts as a substrate adopter for Cullin-dependent E3 ubiquitin ligase complex. Under the condition of oxidative stress, Nrf2 is released from Keap1 and translocates into the nucleus. After heterodimerization with small Maf protein, Nrf2 stimulates the transcription of the downstream genes by binding to antioxidant response element (ARE), a *cis*-acting enhancer with a consensus sequence defined as 5′-TMAnnRTGABnnnGCAwwww-3′, in which the core nucleotide is underlined [16,17]. *tert*-Butylhydroquinone (tBHQ) and sulforaphane (SFN) are known to be representative activators of Nrf2 [18].

There are few reports of the regulatory mechanism of human CES1A. Hosokawa et al. [19] demonstrated that Sp1 and C/EBP are involved in the basal expression of CES1A1. In addition, Nishimura et al. [20] reported that, in human hepatocytes, CES1A mRNA was not induced by rifampicin and omeprazole, which are potent ligands of pregnane X receptor and aryl hydrocarbon receptor (AhR), respectively. Thus, the inducible regulation of CES1A has not been reported until now. Recently, Takakusa et al. [21] reported that CES1A was induced by butylated hydroxyanisole, ticlopidine and diclofenac in human hepatocytes, and that the induction would be stimulated by oxidative stress. As described above, it is well known that Nrf2 is involved in the induction by oxidative stress. In addition, a computer-assisted homology search revealed putative AREs within −3200 bp of the *CES1A1* gene. Thus, it is plausible that Nrf2 is involved in the transcriptional regulation of CES1A. These lines of evidence prompted us to investigate whether the human *CES1A1* gene is regulated by Nrf2.

2. Materials and methods

2.1. Chemicals and reagents

tBHQ was purchased from Wako Pure Chemical Industries (Osaka, Japan). L-SFN was purchased from Alexis (San Diego, CA). Imidapril and imidaprilat were kindly supplied by Mitsubishi Tanabe Pharma Corporation (Osaka, Japan). Anti-human Nrf2 antibodies (C-20 and H-300), which recognize the C- and N-terminus of Nrf2 protein, respectively, were from Santa Cruz Biotechnology (Santa Cruz, CA). Stealth Select RNAi for Nrf2 (HSS107130) (5′-aaucacugaggccaaguaguguguc-3′) and Stealth RNAi negative control, Medium GC Duplex #2 were from Invitrogen (Carlsbad, CA). All primers and oligonucleotides were commercially synthesized at Hokkaido System Sciences (Sapporo, Japan). All other reagents were of the highest grade commercially available.

2.2. Cells and culture conditions

The human hepatoma cell line HepG2 and human colon carcinoma cell line Caco-2 were obtained from American Type Culture Collection (Manassas, VA). Human adenocarcinoma of the cervix of uterus cell line HeLa was obtained from RIKEN BioResource Center (Ibaraki, Japan). HeLa cells were cultured in Dulbecco's modified Eagle's medium (DMEM) (Nissui Pharmaceutical, Tokyo, Japan) supplemented with 10% fetal bovine serum (FBS) (Invitrogen). HepG2 and Caco-2 cells were cultured in DMEM supplemented with 10% FBS and 0.1 mM nonessential amino acids (Invitrogen). The cells were maintained at 37 °C under an atmosphere of 5% CO_2.

2.3. Real-time reverse transcription (RT)-polymerase chain reaction (PCR) analysis

Total RNA was extracted using RNAiso (Takara Bio, Shiga, Japan) and cDNA was synthesized from total RNA using ReverTra Ace (TOYOBO, Osaka, Japan) according to the manufacturer's protocol. Human GAPDH mRNA was quantified by real-time RT-PCR using the Smart Cycler (Cepheid, Sunnyvale, CA) as described previously [22]. CES1A1, CES2 and HO-1 mRNA levels were quantified under the same condition. PCR was performed with the following primer sets: CES1A1, CES1A1 S and CES1A1 AS; CES2, CES2 S and CES2 AS; HO-1, HO-1 S and HO-1 AS (Table 1).

Table 1
Sequences of oligonueleotide used in the present study.

Oligonucleotide	Sequence
For real-time RT-PCR	
CES1A1 S[a]	5′-atgtggctccgtgcct-3′
CES1A1 AS[a]	5′-tcttcacaaagctccatggt-3′
CES2 S[b]	5′-aacctgtctgcctgtgaccaagt-3′
CES2 AS[b]	5′-acatcagcagcgttaacattttctg-3′
HO-1 S[c]	5′-atagagcgaaacaagcaga-3′
HO-1 AS[c]	5′-tagagctgtttgaacttgg-3′
GAPDH S[d]	5′-ccagggctgcttttaactc-3′
GAPDH AS[d]	5′-gctcccccctgcaaatga-3′
For SOE-PCR	
pGL3 S	5′-tagcaaaataggctgtcccc-3′
pGL3 AS	5′-tcgatatgtgcatctgtaaaa-3′
ARE2 mt-A	5′-atctaaggcaaattTTCTTGTCAgctcatt-3′
ARE2 mt-B	5′-aatgagcTGACAAGAAaatttgccttagat-3′
ARE3 mt-A	5′-acagcaactcaatgTTAAAGTCAgaaccag-3′
ARE3 mt-B	5′-ctggttcTGACTTTAAcattgagttgctgt-3′
ARE4 mt-A	5′-cccgtgagattaatTTTGTCTCAcgatctt-3′
ARE4 mt-B	5′-aagatcgTGAGACAAAattaatctcacggg-3′
For ChIP assays	
CES1A1 −2178 S	5′-gaccttaggcaatccctcct-3′
CES1A1 −1855 AS	5′-tggctgtaatcttgtcagtgtttc-3′
CES1A1 −1274 S	5′-tctttgtgtacaagcttttgtg-3′
CES1A1 −956 AS	5′-cacaaggaagtcactcaaag-3′
CES1A1 −958 S	5′-gtgtccccagcagcttgtaa-3′
CES1A1 −666 AS	5′-aaaatgaactccgtcccccc-3′
For electrophoresis mobility shift assays	
cARE[e]	5′-gatcttttatgctgagtcatggttt-3′
CES1A1 ARE4	5′-atttaagatcgTGAGACAGCattaatctc-3′
CES1A1 ARE4mt	5′-atttaagatcgTGAGACAAAattaatctc-3′
CES1A1 ARE6	5′-taggggaattGCTGGGTCAtatggaaactc-3′
CES1A1 ARE6mt	5′-taggggaattTTTGGGTCAtggaaactc-3′

The core ARE is indicated by capital letters and mutated nucleotides are underlined.
[a] From Fukumi et al. [10].
[b] From Sanghani et al. [23].
[c] From Nakamura et al. [24].
[d] From Tsuchiya et al. [22].
[e] From Balogun et al. [12].

2.4. Immunoblot analysis

The expression of CES1A protein was measured by SDS-polyacrylamide gel electrophoresis and immunoblot analysis according to Laemmli [25]. For the preparation of cell homogenates, HepG2 cells were suspended in TGE buffer (10 mM Tris–HCl (pH 7.4), 20% glycerol, 1 mM EDTA) and disrupted by freeze–thawing three times. The protein concentrations were determined according to Bradford [26]. Cell homogenates (30 μg) were separated on 7.5% polyacrylamide gels and electrotransferred onto polyvinylidene difluoride membrane, Immobilon-P (Millipore, Billerica, MA). The membranes were probed with polyclonal rabbit anti-human CES1A (Abcam, Cambridge, MA), and IRDye680-labeled anti-rabbit IgG and an Odyssey infrared imaging system (LI-COR Biosciences, Lincoln, NE) were used for detection. The relative expression level was quantified using ImageQuant TL Image Analysis software (GE Healthcare, Buckinghamshire, UK).

2.5. Imidapril hydrolase activity

The imidapril hydrolase activity was determined according to the method described previously with a slight modification [27]. A

typical standard reaction mixture (total volume, 0.2 ml) contained HepG2 cell homogenates (1 mg/ml), 100 mM Tris–HCl buffer (pH 7.4) and 100 μM imidapril. The final concentration of the organic solvent in the reaction mixture was <1.0%. The reaction was initiated by the addition of imidapril after 2 min of preincubation at 37 °C. After 30 min of incubation, the reaction was terminated by adding 100 μl of ice-cold acetonitrile. After the removal of protein by centrifugation at 9500 × *g* for 5 min, a 10 μl portion of the supernatant was subjected to liquid chromatography-tandem mass spectrometry with an Inertsil ODS-3 analytical column (2.1 mm × 100 mm; GL Science, Tokyo, Japan). The mobile phase consisted of acetonitrile/10 mM ammonium formate (20:80). The mass/charge (*m/z*) ion transitions were recorded in the multiple reaction monitoring mode: *m/z* 378.2 and 206.3 for imidaprilat.

2.6. Construction of reporter plasmid

A pGL3 plasmid containing two copies of the consensus ARE (2× cARE) in the human *NQO-1* gene (5′-gatcagtcacagtgactcagcagaatct-3′), which was previously constructed in our laboratory [24], was used as a positive control. The PCR fragments of the 5′-flanking region (−3207 to −1 bp) in the *CES1A1* gene amplified using genomic DNA samples were cloned into the pGL3-basic vector (Promega, Madison, MI) after treatment with Klenow Fragment (Takara) and digestion with *Xho* I. This plasmid (−3207 to −1 bp) was used for construction of the other reporter plasmids (−1531 to −1, and −833 to −1 bp) by digestion and subcloning. Throughout this article, base A in the initiation codon ATG is denoted +1 and the base before A is numbered −1. Three reporter plasmids containing ARE(s), the −3041 to −2891 bp plasmid that contained ARE1, the −2365 to −1989 bp plasmid that contained ARE2, ARE3 and ARE4, and the −1310 to −1170 bp plasmid that contained ARE5 and ARE6 were constructed by PCR and subcloning. The plasmids mutated at the AREs (ARE2 mt, ARE3 mt and ARE4 mt) were constructed by splicing with overlap extension (SOE)–PCR [28]. The regions around the nucleotides to be mutated were amplified using primer pairs pGL3 S and mt-A (PCR 1), or mt-B and pGL3 AS (PCR 2) (Table 1). The following SOE–PCR was performed with the primer pair pGL3 S and pGL3 AS, combining the PCR products 1 and 2. The SOE–PCR products were digested with the appropriate restriction enzymes and subcloned into the pGL3-tk vector. The nucleotide sequences were confirmed by DNA sequence analysis (Long-Read Tower DNA sequencer; GE Healthcare).

2.7. Transfection and luciferase assay

For siRNA transfection, HepG2, Caco-2 and HeLa cells were transfected with 30 pmol siRNA by using lipofectamine RNAiMAX (Invitrogen). After incubation for 24 h, the cells were treated with 80 μM tBHQ, 10 μM SFN or 0.1% dimethyl sulfoxide (DMSO) for 24 h. For the luciferase assays, HepG2 cells were seeded into 24-well plates at 1 × 10^5 cells/well. Transfection was performed using Tfx-20 reagent (Promega). The transfection mixtures consisted of 200 ng of pGL3 plasmid, 10 ng of phRL-TK plasmid (Promega), and 100 ng of human Nrf2 expression plasmid [24] or pTARGET empty plasmid as a control. The cells were harvested 48 h after transfection and lysed to measure the luciferase activity using a Dual Luciferase Reporter Assay System (Promega). The relative luciferase activities were normalized with the *Renilla* luciferase activities.

2.8. Electrophoretic mobility shift assay (EMSA)

Double-stranded oligonucleotides were labeled with [γ-^{32}P]ATP using T4 polynucleotide kinase (TOYOBO) and purified by Microspin G-50 columns (GE Healthcare). The oligonucleotide sequences are shown in Table 1. The labeled probe (40 fmol, ~20,000 cpm) was applied to each binding reaction in 25 mM HEPES-KOH (pH 7.9), 0.5 mM EDTA (pH 8.0), 10% glycerol, 50 mM KCl, 0.5 mM dithiothreitol, 0.5 mM (*p*-amidinophenyl)methanesulfonyl fluoride, 1 μg of poly(dI-dC), 5 μg of salmon sperm DNA, and 8 μg of the nuclear extracts from 0.1% DMSO- or 10 μM SFN-treated HepG2 cells prepared using NE-PER Nuclear and cytoplasmic extraction reagents (Pierce, Rockford, IL) with a final reaction volume of 15 μl. To determine the specificity of the binding to the oligonucleotides, competition experiments were conducted by co-incubation with 5-, 25-, and 50-fold excesses of unlabeled competitors. For supershift experiments, 2 μg of anti-Nrf2 antibodies (C-20 and H-300) or normal rabbit IgG were preincubated with the nuclear protein on ice for 30 min. The reactions were incubated on ice for 15 min and then loaded on 4% acrylamide gel in 0.5× Tris–borate EDTA buffer. The gels were dried and exposed to film for 24 h. The DNA–protein complexes were detected with a Fuji Bio-Imaging Analyzer BAS 1800 (Fuji Film, Tokyo, Japan).

2.9. Chromatin immunoprecipitation (ChIP) assay

When HepG2 cells reached 60% confluence in 60-mm dishes, they were treated with 0.1% DMSO or 10 μM SFN. After 24 h incubation, ChIP assays were performed using a ChIP assay kit (Upstate, Lake Placid, NY) according to the manufacturer's protocol. Rabbit anti-Nrf2 antibodies (C-20 and H-300) and normal rabbit IgG were used for immunoprecipitation of the protein–DNA complexes. PCR was performed with the following primer sets: region 1, CES1A1 −2178 S and CES1A1 −1855 AS; region 2, CES1A1 −1274 S and CES1A1 −956 AS; region 3, CES1A1 −956 S and CES1A1 −666 AS (Table 1). The PCR conditions were as follows: after initial denaturation at 94 °C for 3 min, the amplification was performed by denaturation at 94 °C for 25 s, annealing at 58 °C (region 1), 54 °C (region 2) or 60 °C (region 3) for 25 s, and extension at 72 °C for 30 s for 30 cycle. The PCR products were electrophoresed on a 2% agarose gel and visualized by ethidium bromide.

2.10. Statistical analysis

Data are expressed as mean ± SD. Statistical significance between two groups was determined by two-tailed Student's *t*-test. Statistical significance between multiple groups was determined by ANOVA followed by Dunnett or Tukey test. A value of $P < 0.05$ was considered statistically significant.

3. Results

3.1. Induction of CES1A in cultured cells

The effects of tBHQ and SFN on the expression of CES1A1 mRNA in HepG2, Caco-2 and HeLa cells were examined (Fig. 1). By treatment with 80 μM tBHQ and 10 μM SFN, the expression of CES1A1 mRNA was significantly increased in HepG2 (2.6- and 3.4-fold, respectively), Caco-2 (3.4- and 4.4-fold) and HeLa cells (3.4- and 3.0-fold). Under the same condition, the level of HO-1 mRNA, which is already known to be induced by Nrf2, was also significantly induced in all cell lines. In contrast, the level of CES2 mRNA was not changed in any of cell lines. The CES1A protein expression and enzyme activity were measured to examine whether they were increased by the induction of CES1A1 mRNA expression by tBHQ and SFN in HepG2 cells. Immunoblot analysis revealed that the expression of CES1A protein was clearly increased up to 1.73- and 2.12-fold in HepG2 cells by tBHQ and SFN, respectively (Fig. 1B). In Caco-2 and HeLa cells, it was difficult to detect CES1A protein by immunoblot analysis due to the

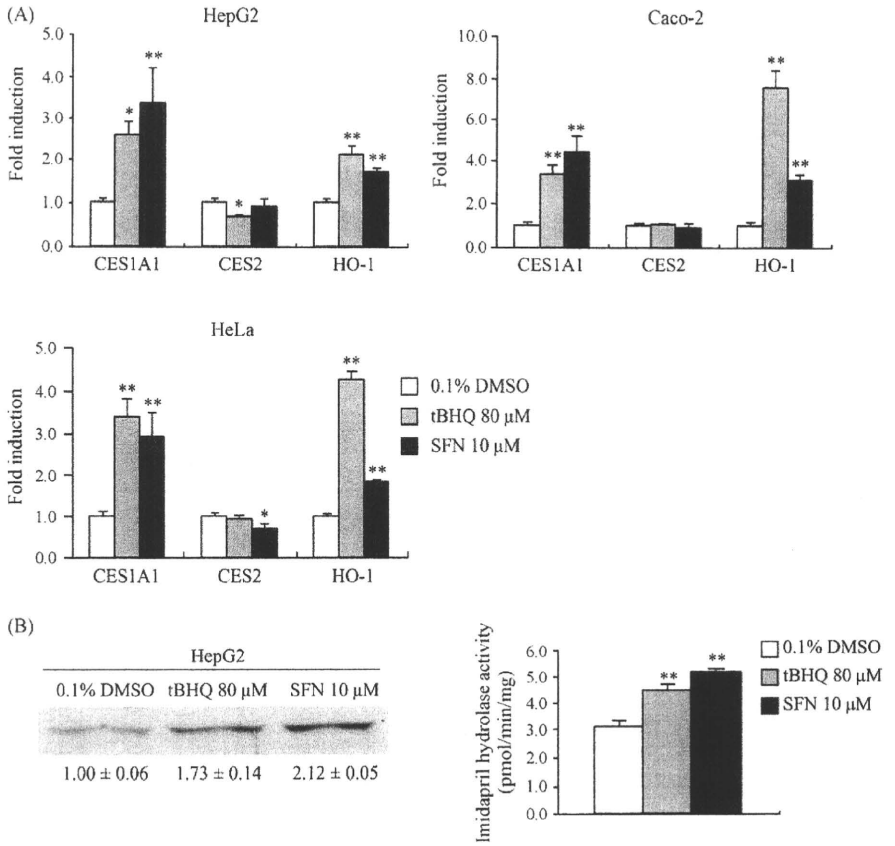

Fig. 1. (A) Effects of tBHQ and SFN on the CES1A1, CES2 and HO-1 mRNA expression in HepG2, Caco-2, and HeLa cells. The cells were treated with 80 μM tBHQ, 10 μM SFN or DMSO vehicle (0.1%) for 24 h. The expressions of CES1A1, CES2 and HO-1 mRNA were determined by real-time RT-PCR and normalized with the GAPDH mRNA levels. Effects of tBHQ and SFN on the expression of CES1A protein (B) and the imidapril hydrolase activity (C) in HepG2 cells. The cells were treated with 80 μM tBHQ, 10 μM SFN or DMSO vehicle (0.1%) for 24 h. The expression of CES1A protein was determined by immunoblot analysis. Each column represents the mean ± SD of three independent experiments. $^{*}P < 0.05$; $^{**}P < 0.01$ compared with control (vehicle).

low expression level. Imidapril hydrolase activity, which is specifically catalyzed by CES1A, was also significantly increased in HepG2 cells by tBHQ and SFN (from 3.4 ± 0.23 to 4.13 ± 0.23 and 5.31 ± 0.15 pmol/min/mg protein, respectively) (Fig. 1C). These results indicate that the induction of CES1A1 mRNA expression by tBHQ and SFN led to increases in CES1A protein expression and enzyme activity.

3.2. Effect of Nrf2 knockdown on the induction of CES1A1 by tBHQ and SFN

To investigate whether Nrf2 is responsible for the induction of CES1A1 by tBHQ and SFN, the endogenous Nrf2 was knockdowned in HepG2, Caco-2 and HeLa cells (Fig. 2). It was confirmed that the Nrf2 mRNA expression was decreased 79%, 82%, and 88% by siRNA-Nrf2 transfection in HepG2, Caco-2, and HeLa cells, respectively. In all cell lines, tBHQ and SFN mediated induction of CES1A1 mRNA was completely suppressed by the knockdown of Nrf2. In HepG2 and Caco-2 cells, the basal expression level of CES1A1 mRNA was not changed by siRNA-Nrf2 transfection, whereas it was significantly decreased in HeLa cells. These results suggested that Nrf2 plays a critical role in the induction of CES1A1 by tBHQ and SFN.

3.3. Identification of Nrf2 binding site in the 5′-flanking region of the CES1A1 gene

A computer-assisted homology search identified six putative AREs within −3200 bp of the *CES1A1* gene (Fig. 3). These AREs at −2971, −2323, −2203, −2025, −1283, and −1218 bp were termed ARE1, ARE2, ARE3, ARE4, ARE5 and ARE6, respectively. To investigate whether AREs in the *CES1A1* gene were functional in Nrf2-dependent transactivation, luciferase assays were performed using reporter plasmids containing the 5′-flanking region of the *CES1A1* gene (−3207 to −1, −1531 to −1, and −833 to −1 bp) in HepG2 cells (Fig. 4A). The transcriptional activity of 2× cARE used as positive control was increased up to 2.2-fold by the overexpression of Nrf2. Unexpectedly, the overexpression of Nrf2 did not activate the transcriptional activities of any plasmids. Then, we constructed three reporter plasmids containing ARE-neighboring regions and luciferase assays were performed (Fig. 4B). The transcriptional activities of the −2365 to −1989 bp plasmid that contained ARE2, ARE3 and ARE4 were increased up to 2.0-fold by the overexpression of Nrf2. In contrast, Nrf2 did not activate the transcriptional activities of the −3041 to −2891 bp plasmid that contained ARE1 and the −1310 to −1170 bp plasmid that contained ARE5 and ARE6. To further confirm the functional ARE, a mutation was introduced into each ARE of the −2365 to −1989 bp plasmid. The Nrf2-dependent transcriptional activation with the −2365 to −1989 bp plasmid was completely abolished by introducing the mutation in ARE4 (Fig. 4C). These results suggest that the ARE4 works as a functional Nrf2 response element in the *CES1A1* gene.

3.4. Nrf2 directly binds to the ARE at −2025 of the CES1A1 gene

To examine whether Nrf2 directly binds to ARE4, EMSA was performed using the nuclear extract prepared from DMSO- or SFN-treated HepG2 cell and ^{32}P-labeled ARE4 as a probe (Fig. 5). When

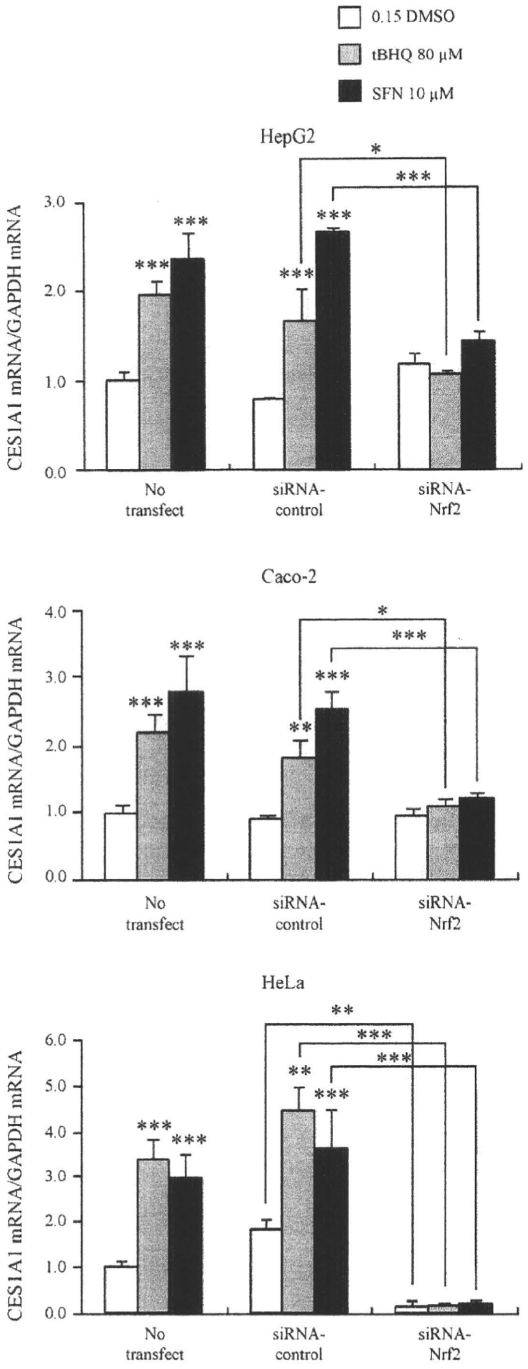

Fig. 2. Effect of Nrf2 knockdown on CES1A1 mRNA induction in HepG2, Caco-2 and HeLa cells. The expression of CES1A1 mRNA was determined by real-time RT-PCR. After 24 h transfection with siRNA, the cells were treated with 80 μM tBHQ, 10 μM SFN or DMSO vehicle (0.1%) for 24 h. To normalize RNA loading and PCR variations, the CES1A1 mRNA levels were corrected with the GAPDH mRNA levels. Each column represents the mean ± SD of three independent experiments. $^{*}P < 0.05$; $^{**}P < 0.01$; $^{***}P < 0.001$ compared with control (vehicle).

the probe was incubated with the nuclear extracts from the SFN-treated HepG2 cells, the shifted band was clearly observed. The band density was diminished with both anti-Nrf2 antibodies (C-20 and H-300), although the supershifted band was observed only with the anti-Nrf2 antibody (C-20). These results indicate that the shifted band contained Nrf2 complexes. Moreover, the shifted

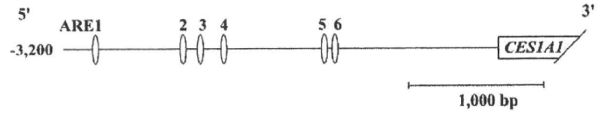

Consensus ARE		TMAnnRTGABnnnGCAwwww	
ARE1	-2,984	TcAgaGCATCcTCATTCccA	-2,965
ARE2	-2,329	atgAGcTGACAAGGCAATTT	-2,310
ARE3	-2,209	TggTTcTGACTTTGCcATTg	-2,190
ARE4	-2,031	agATCGTGAgACAGCATTAA	-2,012
ARE5	-1,289	gATGAATGACACTGCtcTTT	-1,270
ARE6	-1,193	gAATTGCTGGGTCAATATgG	-1,212

Fig. 3. Schematic diagram of putative AREs in the 5′-flanking region of the human *CES1A1* gene. Numbers indicate the nucleotide position when the A in the initiation codon ATG is denoted +1 and the base before A is numbered −1. The core ARE sequence is indicated by an arrow. The nucleotides that are consistent with the consensus ARE are shown with capital letters.

band was competed out by excess amounts of unlabeled cARE or ARE4, but not by the mutant ARE, ARE4 mt. These results suggested that Nrf2 binds to the ARE located at −2025 in the 5′-flanking region of the *CES1A1* gene.

To further examine whether Nrf2 binds to ARE4 in intact cells, ChIP assays were performed using DMSO- or SFN-treated HepG2 cells (Fig. 6). PCR was performed with primers designed to amplify the −2178 to −1855 bp (region 1) containing ARE4, the −1274 to −956 bp (region 2) containing ARE6 and the −958 to −666 bp (region 3) containing no AREs. Normal rabbit IgG was used as a negative control of immunoprecipitation for ChIP assays. As shown in Fig. 6, the immunoprecipitants of SFN-treated HepG2 cells obtained with anti-Nrf2 antibody (C-20) generated a distinct PCR product for region 1, but those obtained with anti-Nrf2 antibody (H-300) or normal rabbit IgG did not. Using primer sets for region 2 and region 3, no PCR products were obtained with any antibodies. These results suggest that Nrf2 binds to the ARE located at −2025 in the 5′-flanking region of the *CES1A1* gene in intact cells.

4. Discussion

In this study, we demonstrated that human CES1A1 is induced by Nrf2. The human *CES1A1* gene and *CES1A3* pseudogene are inverted and duplicated genes. Our recent study demonstrated that the *CES1A2* gene is a variant of the *CES1A3* pseudogene [10]. In the present study, we demonstrated that the ARE4 in the *CES1A1* gene was the key element of Nrf2-mediated induction, but the sequence of the region corresponding to ARE4 in the *CES1A1* gene exists in the *CES1A2* gene. Therefore, it is conceivable that CES1A2 mRNA derived from the *CES1A2* gene is also induced by Nrf2. The copy numbers of the *CES1A2* gene and *CES1A3* pseudogene were investigated for HepG2, Caco-2 and HeLa cells according to Fukami et al. [10] (data not shown). HepG2 and Caco-2 cells had two copies of the *CES1A3* gene, but HeLa cells had one copy each of the *CES1A3* and *CES1A2* genes. However, in HeLa cells, CES1A2 mRNA was not detected (data not shown), thus the induction of CES1A2 by Nrf2 could not be further investigated. Since the expression of CES1A2 mRNA is much lower than that of CES1A1 mRNA in human liver [10], the Nrf2-mediated induction of CES1A2 would have a minor effect on the CES1A enzyme activity.

NQO1, HO-1, and UGT1A1 are well known to be induced by tBHQ and SFN via Nrf2 [11–13]. Recently, these inductions have attracted attention as biomarkers of the electrophilic stress caused by the formation of reactive metabolites because they serve as a cellular defense against electrophiles and oxidative stress products [29]. It is plausible that CES1A1 is also a possible biomarker of

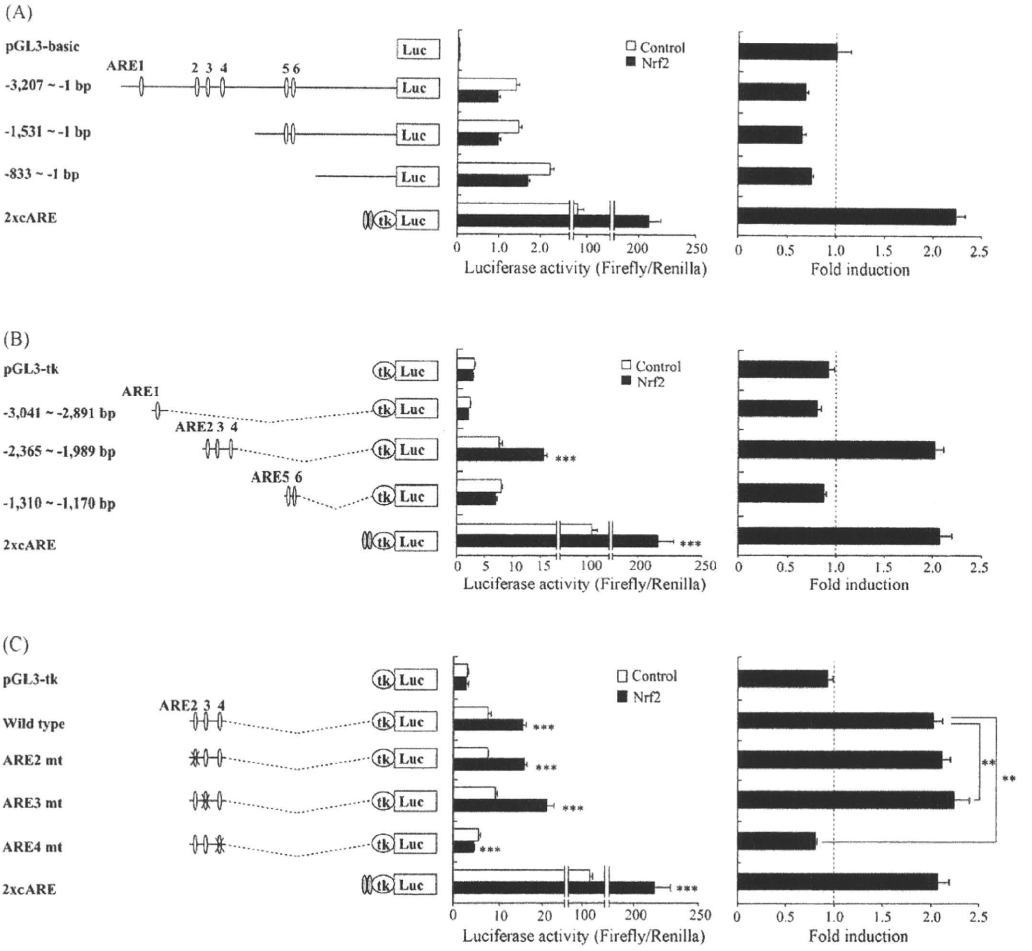

Fig. 4. Relative promoter activity of constructs containing putative ARE(s) in the 5′-flanking region of the *CES1A1* gene and the effect of the overexpression of Nrf2 in HepG2 cells. After 48 h transfection, the cells were harvested and assayed for the luciferase activities according to the manufacturer's protocol. The relative luciferase activities were normalized with the *Renilla* luciferase activities. The right part of the figure shows the fold induction of the transcriptional activity by the overexpression of Nrf2. Each column represents the mean ± SD of three independent experiments. 2×cARE indicates the plasmid containing two copies of the consensus ARE in the human NQO-1 gene. ARE2 mt, AER3 mt, ARE4 mt indicate the plasmids mutated at the ARE2, ARE3, and ARE4, respectively. Control, pTARGET empty plasmid. $^{**}P < 0.01$ and $^{***}P < 0.001$.

electrophilic stress because it was demonstrated in this study that CES1A1 is induced by Nrf2. tBHQ and SFN are also known as ligands of AhR [30,31]. NQO1, HO-1, and UGT1A1 are induced by AhR as well as by Nrf2 [32–34]. In the present study, CES1A1 induction by tBHQ and SFN was completely suppressed by knockdown of Nrf2. In addition, it was reported that CES1A mRNA is not induced by omeprazole, a potent ligand of AhR, in human hepatocytes [20]. These results indicate that only Nrf2 but not AhR would be involved in the CES1A1 induction by tBHQ and SFN. Interestingly, in HeLa cells, the basal expression level of CES1A1 mRNA was significantly decreased by the knockdown of Nrf2. This result indicates that Nrf2 regulates the basal expression of CES1A1 in HeLa cells. Similarly, it was reported that the basal expression level of carboxylesterase in lung and small intestine is decreased in Nrf2 knockout mice [35,36]. In addition to Sp1 and C/EBP [19], Nrf2 might also regulate the basal expression level of CES1A1.

Generally, the genes induced by Nrf2 are involved in detoxification [18]. Because CES1A expression was induced by Nrf2, it was conceivable that CES1A is also involved in detoxification. It was reported that carboxylesterase in human lung microsomes, in which CES1A is highly expressed, is involved in the detoxification of vinyl carbamate [37]. To our knowledge, this is the only report suggesting the involvement of CES1A in the detoxification of reactive intermediates and carcinogens. It appears that CES1A is associated with lipid elimination in the liver [4–6]. Oxidative stress is one of the causal factors for hepatic steatosis, which leads to liver injury [38]. Although there were no reports about the relevance of CES1A to hepatic steatosis, CES1A may be involved in the defense of the cells against hepatic steatosis.

As shown in Fig. 4B, the transcriptional activities using the plasmid containing sequence −2365 to −1989 in the 5′-flanking region of the *CES1A1* gene were increased up to 2.0-fold by overexpression of Nrf2, and it was demonstrated that the ARE4 works as a functional Nrf2 response element in the *CES1A1* gene. Although we analyzed the transcriptional activity using plasmids containing the sequences −3207 to −1, −1531 to −1, and −833 to −1 bp in the 5′-flanking region of the *CES1A1* gene, the activity was not increased by the overexpression of Nrf2 (Fig. 4A). This result was similar to that in our previous study in which a significant increase of the transcriptional activity by Nrf2 overexpression was not observed using plasmids containing the sequences −2191 or −1408 to −7 in the 5′-flanking region of the *UGT2B7* gene [24]. It is assumed that the plasmid containing the long sequence results in a complicated conformation, which makes it difficult for Nrf2 to bind to the target ARE.

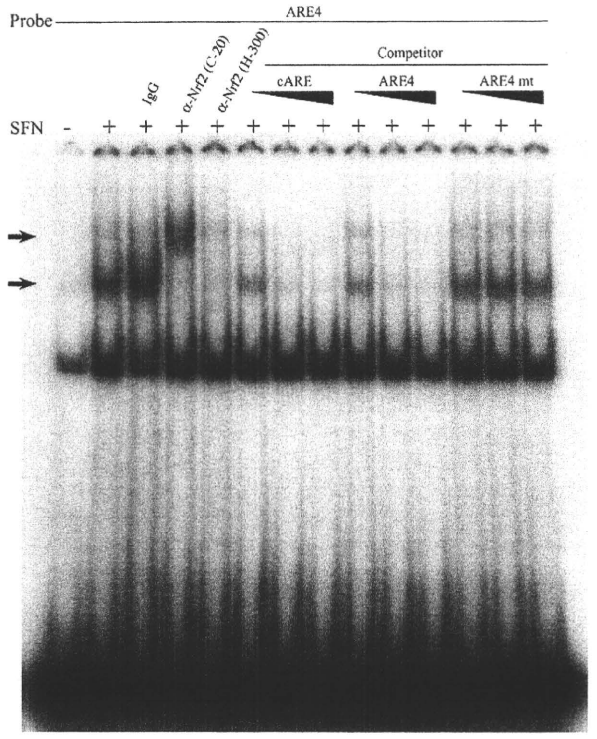

Fig. 5. Electrophoretic mobility shift assays of Nrf2 binding to ARE4 in the *CES1A1* gene. Oligonucleotide probes of CES1A1 ARE4 labeled with ^{32}P were incubated with nuclear extracts prepared from HepG2 cells treated with 10 μM SFN or DMSO vehicle (0.1%). The sequences of the oligonucleotides are shown in Table 1. Cold oligonucleotides were used as a competitor at 5-, 25-, and 50-fold molar excess. For supershift analyses, 2 μg of anti-Nrf2 antibodies (α-Nrf2) or normal rabbit IgG (IgG) were preincubated with the nuclear extracts on ice for 30 min. The *lower* arrow indicates the position of the Nrf2-dependent shifted band, and the *upper* one indicates the supershifted complex by anti-Nrf2 antibodies.

EMSA and ChIP assays revealed that Nrf2 binds to the 5′-flanking region in the *CES1A1* gene (Figs. 5 and 6). In EMSA, the supershifted band was observed only with the anti-Nrf2 antibody (C-20) but not with the anti-Nrf2 antibody (H-300). This result is consistent with our previous study [24]. In ChIP assays, the

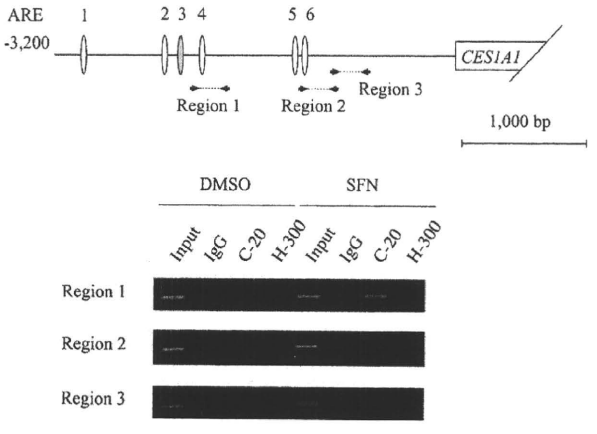

Fig. 6. ChIP assays of Nrf2 binding to the *CES1A1* gene in HepG2 cells. Schematic diagram of the *CES1A1* gene is shown at the top. ChIP assays were performed as described in Section 2. HepG2 cells were treated with 10 μM SFN or DMSO vehicle (0.1%) for 24 h. Rabbit anti-Nrf2 antibodies (C-20 and H-300) and normal rabbit IgG were used for immunoprecipitation of protein–DNA complexes. DNA fragments amplified by PCR were analyzed on 2% agarose gel.

immunoprecipitants of SFN-treated HepG2 cells obtained with anti-Nrf2 antibody (C-20) generated PCR products for region 1 containing functional ARE, but those obtained with anti-Nrf2 antibody (H-300) or normal rabbit IgG did not. Anti-Nrf2 antibody (C-20) recognizes the C-terminal of Nrf2, whereas anti-Nrf2 antibody (H-300) recognizes the N-terminal. This difference in the recognition sites between anti-Nrf2 antibodies (C-20 and H-300) may affect the results in EMSA and the ChIP assays.

Deng et al. [39] and Wu et al. [40] reported that the cholesterol-lowering drug probucol induces HO-1 via oxidative stress. Aburaya et al. [41] reported that Nrf2 is activated by non-steroidal anti-inflammatory drugs (NSAIDs), such as indomethacin, diclofenac, ibuprofen and aspirin. Moreover, isothiocyanates such as SFN and phenethyl isothiocyanate are found broadly distributed among cruciferous vegetables, e.g., cabbage and broccoli. It was reported that the intake of cruciferous vegetables for 2 weeks lowers serum bilirubin concentrations (from 15.73 to 14.02 μmol/L) by up-regulating UGT1A1 activity [42]. In human skin, NQO1 activity is induced up to 1.5-fold by sulforaphane-containing broccoli sprouts [43]. Because CES1A is involved in the metabolism of a number of clinically used drugs and prodrugs, the combined use of drugs or dietary foods that activate Nrf2 might affect the drug response.

In conclusion, we found that Nrf2 transcriptionally activates CES1A1 through binding to the ARE in the 5′-flanking region. This is the first study to demonstrate the molecular mechanism of the inducible regulation of human CES1A1.

Acknowledgement

We acknowledge Mr. Brent Bell for reviewing the manuscript.

References

[1] Song JC, White CM. Clinical pharmacokinetics and selective pharmacodynamics of new angiotensin converting enzyme inhibitors: an update. Clin Pharmacokinet 2002;41:207–24.
[2] Shi D, Yang J, Yang D, LeCluyse EL, Black C, You L, et al. Anti-influenza prodrug oseltamivir is activated by carboxylesterase human carboxylesterase 1, and the activation is inhibited by antiplatelet agent clopidogrel. J Pharmacol Exp Ther 2007;319:1477–84.
[3] Humerickhouse R, Lohrbach K, Li L, Bosron WF, Dolan ME. Characterization of CPT-11 hydrolysis by human liver carboxylesterase isoforms hCE-1 and hCE-2. Cancer Res 2000;60:1189–92.
[4] Pindel EV, Kedishvili NY, Abraham TL, Brzezinski MR, Zhang J, Dean RA, et al. Purification and cloning of a broad substrate specificity human liver carboxylesterase that catalyzes the hydrolysis of cocaine and heroin. J Biol Chem 1997;272:14769–75.
[5] Dolinsky VW, Gilham D, Alam M, Vance DE, Lehner R. Triacylglycerol hydrolase: role in intracellular lipid metabolism. Cell Mol Life Sci 2004;61:1633–51.
[6] Becker A, Böttcher A, Lackner KJ, Fehringer P, Notka F, Aslanidis C, et al. Purification, cloning, and expression of a human enzyme with acyl coenzyme A: cholesterol acyltransferase activity, which is identical to liver carboxylesterase. Arterioscler Thromb 1994;14:1346–55.
[7] Zhao B, Natarajan R, Ghosh S. Human liver cholesteryl ester hydrolase: cloning, molecular characterization, and role in cellular cholesterol homeostasis. Physiol Genomics 2005;23:304–10.
[8] Satoh T, Taylor P, Bosron WF, Sanghani SP, Hosokawa M, La Du BN. Current progress on esterases: from molecular structure to function. Drug Metab Dispos 2002;30:488–93.
[9] Hosokawa M, Furihata T, Yaginuma Y, Yamamoto N, Koyano N, Fujii A, et al. Genomic structure and transcriptional regulation of the rat, mouse, and human carboxylesterase genes. Drug Metab Rev 2007;39:1–15.
[10] Fukami T, Nakajima M, Maruichi T, Takahashi S, McLeod HL, Takamiya M, et al. Structure and characterization of human carboxylesterase 1A1, 1A2, and 1A3 genes. Pharmacogenet Genomics 2008;18:911–20.
[11] Nioi P, McMahon M, Itoh K, Yamamoto M, Hayes JD. Identification of a novel Nrf2-regulated antioxidant response element (ARE) in the mouse NAD(P)H:-quinone oxidoreductase 1 gene: reassessment of the ARE consensus sequence. Biochem J 2003;374:337–48.
[12] Balogun E, Hoque M, Gong P, Killeen E, Green CJ, Foresti R, et al. Curcumin activates the haem oxygenase-1 gene via regulation of Nrf2 and the antioxidant-responsive element. Biochem J 2003;371:887–95.
[13] Yueh MF, Tukey RH. Nrf2-Keap1 signaling pathway regulates human UGT1A1 expression in vitro and in transgenic UGT1 mice. J Biol Chem 2007;282:8749–58.

[14] Moi P, Chan K, Asunis I, Cao A, Kan YW. Isolation of NF-E2-related factor 2 (Nrf2), a NF-E2-like basic leucine zipper transcriptional activator that binds to the tandem NF-E2/AP1 repeat of the β-globin locus control region. Proc Natl Acad Sci USA 1994;91:9926–30.
[15] Motohashi H, O'Connor T, Katsuoka F, Engel JD, Yamamoto M. Integration and diversity of the regulatory network composed of Maf and CNC families of transcription factors. Gene 2002;294:1–12.
[16] Nerland DE. The antioxidant/electrophile response element motif. Drug Metab Rev 2007;39:235–48.
[17] Itoh K, Chiba T, Takahashi S, Ishii T, Igarashi K, Katoh Y, et al. An Nrf2/small Maf heterodimer mediates the induction of phase II detoxifying enzyme genes through antioxidant response elements. Biochem Biophys Res Commun 1997;236:313–22.
[18] Li W, Kong AN. Molecular mechanisms of Nrf2-mediated antioxidant response. Mol Carcinog 2009;48:91–104.
[19] Hosokawa M, Furihata T, Yaginuma Y, Yamamoto N, Watanabe N, Tsukada E, et al. Structural organization and characterization of the regulatory element of the human carboxylesterase (CES1A1 and CES1A2) genes. Drug Metab Pharmacokinet 2008;23:73–84.
[20] Nishimura M, Imai T, Morioka Y, Kuribayashi S, Kamataki T, Naito S. Effects of NO-1886 (Ibrolipim), a lipoprotein lipase-promoting agent, on gene induction of cytochrome P450s, carboxylesterases, and sulfotransferases in primary cultures of human hepatocytes. Drug Metab Pharmacokinet 2004;19:422–9.
[21] Takakusa H, Masumoto H, Mitsuru A, Okazaki O, Sudo K. Markers of electrophilic stress caused by chemically reactive metabolites in human hepatocytes. Drug Metab Dispos 2008;36:816–23.
[22] Tsuchiya Y, Nakajima M, Kyo S, Kanaya T, Inoue M, Yokoi T. Human CYP1B1 is regulated by estradiol via estrogen receptor. Cancer Res 2004;64:3119–25.
[23] Sanghani SP, Quinney SK, Fredenburg TB, Sun Z, Davis WI, Murry DJ, et al. Carboxylesterases expressed in human colon tumor tissue and their role in CPT-11 hydrolysis. Clin Cancer Res 2003;9:4983–91.
[24] Nakamura A, Nakajima M, Higashi E, Yamanaka H, Yokoi T. Genetic polymorphisms in the 5′-flanking region of human UDP-glucuronosyltransferase 2B7 affect the Nrf2-dependent transcriptional regulation. Pharmacogenet Genomics 2008;18:709–20.
[25] Laemmli UK. Cleavage of structural proteins during the assembly of the head of bacteriophage T4. Nature 1970;227:680–5.
[26] Bradford MM. A rapid and sensitive method for the quantitation of microgram quantities of protein utilizing the principle of protein-dye binding. Anal Biochem 1976;72:248–54.
[27] Takahashi S, Katoh M, Saitoh T, Nakajima M, Yokoi T. Allosteric kinetics of human carboxylesterase1: species difference and interindividual variability. J Pharm Sci 2008;97:5434–45.
[28] Horton RM, Cai ZL, Ho SN, Pease LR. Gene splicing by overlap extension: tailor-made genes using the polymerase chain reaction. Biotechniques 1990;8:528–35.
[29] Zhang DD. Mechanistic studies of the Nrf2-Keap1 signaling pathway. Drug Metab Rev 2006;38:769–89.
[30] Gharavi N, El-Kadi AO. tert-Butylhydroquinone is a novel aryl hydrocarbon receptor ligand. Drug Metab Dispos 2005;33:365–72.
[31] Anwar-Mohamed A, El-Kadi AO. Sulforaphane induces CYP1A1 mRNA, protein, and catalytic activity levels via an AhR-dependent pathway in murine hepatoma Hepa 1c1c7 and human HepG2 cells. Cancer Lett 2009;275:93–101.
[32] Marchand A, Barouki R, Garlatti M. Regulation of NAD(P)H:quinone oxidoreductase 1 gene expression by CYP1A1 activity. Mol Pharmacol 2004;65:1029–37.
[33] Elbekai RH, El-Kadi AO. Transcriptional activation and posttranscriptional modification of Cyp1a1 by arsenite, cadmium, and chromium. Toxicol Lett 2007;172:106–19.
[34] Sugatani J, Mizushima K, Osabe M, Yamakawa K, Kakizaki S, Takagi H, et al. Transcriptional regulation of human UGT1A1 gene expression through distal and proximal promoter motifs: implication of defects in the UGT1A1 gene promoter. Naunyn Schmiedebergs Arch Pharmacol 2008;377:597–605.
[35] Thimmulappa RK, Mai KH, Srisuma S, Kensler TW, Yamamoto M, Biswal S. Identification of Nrf2-regulated genes induced by the chemopreventive agent sulforaphane by oligonucleotide microarray. Cancer Res 2002;62:5196–203.
[36] Cho HY, Reddy SP, Yamamoto M, Kleeberger SR. The transcription factor NRF2 protects against pulmonary fibrosis. FASEB J 2004;18:1258–60.
[37] Forkert PG, Lee RP, Reid K. Involvement of CYP2E1 and carboxylesterase enzymes in vinyl carbamate metabolism in human lung microsomes. Drug Metab Dispos 2001;29:258–63.
[38] Vidali M, Tripodi MF, Ivaldi A, Zampino R, Occhino G, Restivo L, et al. Interplay between oxidative stress and hepatic steatosis in the progression of chronic hepatitis C. J Hepatol 2008;48:399–406.
[39] Deng YM, Wu BJ, Witting PK, Stocker R. Probucol protects against smooth muscle cell proliferation by upregulating heme oxygenase-1. Circulation 2004;110:1855–60.
[40] Wu BJ, Kathir K, Witting PK, Beck K, Choy K, Li C, et al. Antioxidants protect from atherosclerosis by a heme oxygenase-1 pathway that is independent of free radical scavenging. J Exp Med 2006;203:1117–27.
[41] Aburaya M, Tanaka K, Hoshino T, Tsutsumi S, Suzuki K, Makise M, et al. Heme oxygenase-1 protects gastric mucosal cells against non-steroidal anti-inflammatory drugs. J Biol Chem 2006;281:33422–32.
[42] Navarro SL, Peterson S, Chen C, Makar KW, Schwarz Y, King IB, et al. Cruciferous vegetable feeding alters UGT1A1 activity: diet- and genotype-dependent changes in serum bilirubin in a controlled feeding trial. Cancer Prev Res (Phila Pa) 2009;2:345–52.
[43] Dinkova-Kostova AT, Fahey JW, Wade KL, Jenkins SN, Shapiro TA, Fuchs EJ, et al. Induction of the phase 2 response in mouse and human skin by sulforaphane-containing broccoli sprout extracts. Cancer Epidemiol Biomarkers Prev 2007;16:847–51.

Interactions Between Human UDP-Glucuronosyltransferase (UGT) 2B7 and UGT1A Enzymes

RYOICHI FUJIWARA,[1] MIKI NAKAJIMA,[1] SHINGO ODA,[1] HIROYUKI YAMANAKA,[1] SHIN-ICHI IKUSHIRO,[2] TOSHIYUKI SAKAKI,[2] TSUYOSHI YOKOI[1]

[1]Drug Metabolism and Toxicology, Faculty of Pharmaceutical Sciences, Kanazawa University, Kakuma-machi, Kanazawa 920-1192, Japan

[2]Food Science and Technology, Biotechnology Research Center, Faculty of Engineering, Toyama Prefectural University, Toyama, Japan

Received 16 February 2009; revised 23 April 2009; accepted 28 April 2009

Published online 27 May 2009 in Wiley InterScience (www.interscience.wiley.com). DOI 10.1002/jps.21830

ABSTRACT: Glucuronidation catalyzed by UDP-glucuronosyltransferase (UGT) enzymes is an important pathway in the metabolism of drugs as well as environmental chemicals. In this study, protein–protein interactions between human UGT2B7 and UGT1As and their effects on the enzymatic activities were investigated using double expression systems in HEK293 cells (UGT2B7/UGT1A1, UGT2B7/UGT1A4, UGT2B7/UGT1A6, and UGT2B7/UGT1A9). Native-PAGE analysis clearly revealed that UGT2B7 forms homo-oligomers. Furthermore, hetero-oligomers of UGT2B7 with UGT1As were observed by native-PAGE analysis. Immunoprecipitation assay revealed associations of UGT2B7 with UGT1A1, UGT1A4, UGT1A6, and UGT1A9. The thermal stability of UGT2B7 was significantly increased by the coexpressed UGT1A1, UGT1A4, UGT1A6, and UGT1A9, indicating an interaction between UGT2B7 and the UGT1As. To examine the effects of the protein–protein interactions on the enzymatic activities, kinetic analyses were performed. Coexpression of the UGT1As significantly decreased K_m and increased V_{max} of zidovudine *O*-glucuronidation by UGT2B7. Coexpression of UGT2B7 also affected the kinetics of estradiol 3-*O*-glucuronidation by UGT1A1, imipramine *N*-glucuronidation by UGT1A4, serotonin *O*-glucuronidation by UGT1A6, and propofol *O*-glucuronidation by UGT1A9. In conclusion, it was clearly demonstrated that human UGT2B7 interacts with UGT1A enzymes, affecting their kinetics. That such interactions might occur in human liver microsomes underscores the complexities in glucuronidations in human liver. © 2009 Wiley-Liss, Inc. and the American Pharmacists Association J Pharm Sci 99:442–454, 2010

Keywords: hepatic metabolism; enzyme kinetics; phase II enzymes; glucuronosyltransferases (UGT); metabolic clearance

INTRODUCTION

UDP-Glucuronosyltransferases (UGTs) catalyze the conjugation of endogenous and exogenous compounds with UDP-glucuronic acid (UDPGA).[1] Human UGTs are classified into three subfamilies, UGT1A, UGT2A, and UGT2B, based on evolutionary divergence.[2] The human *UGT1A* gene cluster located on chromosome 2q37 contains multiple unique first exons for each UGT1A, with exons 2–5 in common,[3] encoding nine kinds of functional UGT1As. The *UGT2A* and *UGT2B* genes are located on chromosome 4q13, encoding three and seven functional proteins, respectively. UGT2A1 and UGT2A2 are formed by differential splicing of variable first exons and the common

Abbreviations: UGT, UDP-glucuronosyltransferase; UDPGA, UDP-glucuronic acid; HPLC, high performance liquid chromatography.

Correspondence to: Tsuyoshi Yokoi (Telephone: 81-76-234-4407; Fax: 81-76-234-4407;
E-mail: tyokoi@kenroku.kanazawa-u.ac.jp)

Journal of Pharmaceutical Sciences, Vol. 99, 442–454 (2010)